NASA TECHNICAL MEMORANDUM

NASA TM X-2879

NASA TM X-2879

CONTROL OF SUPERSONIC WIND-TUNNEL NOISE BY LAMINARIZATION OF NOZZLE-WALL BOUNDARY LAYERS

by Ivan E. Beckwith, William D. Harvey, Julius E. Harris, and Barbara B. Holley

Langley Research Center
Hampton, Va. 23665

NATIONAL AERONAUTICS AND SPACE ADMINISTRATION • WASHINGTON, D. C. • DECEMBER 1973

1. Report No.	2. Government Accession No.	3. Recipient's Catalog No.
NASA TM X-2879		

4. Title and Subtitle	5. Report Date
CONTROL OF SUPERSONIC WIND-TUNNEL NOISE BY LAMINARIZATION OF NOZZLE-WALL BOUNDARY LAYERS	December 1973
	6. Performing Organization Code

7. Author(s)	8. Performing Organization Report No.
Ivan E. Beckwith, William D. Harvey, Julius E. Harris, and Barbara B. Holley	L-9090
	10. Work Unit No. 501-06-07-03
9. Performing Organization Name and Address	11. Contract or Grant No.
NASA Langley Research Center Hampton, Va. 23665	
	13. Type of Report and Period Covered
12. Sponsoring Agency Name and Address	Technical Memorandum
National Aeronautics and Space Administration Washington, D.C. 20546	14. Sponsoring Agency Code

15. Supplementary Notes

Appendix by P. Calvin Stainback, William D. Harvey, and John B. Anders.

16. Abstract

One of the principal design requirements for a "quiet" supersonic or hypersonic wind tunnel is to maintain laminar boundary layers on the nozzle walls and thereby reduce disturbance levels in the test flow. The purpose of this report is to review the conditions and apparent reasons for laminar boundary layers which have been observed during previous investigations on the walls of several nozzles for exit Mach numbers from 2 to 20.

Based on these results, an analysis and an assessment of nozzle design requirements for laminar boundary layers including low Reynolds numbers, high acceleration, suction slots, wall temperature control, wall roughness, and area suction are presented.

17. Key Words (Suggested by Author(s))	18. Distribution Statement
Wind-tunnel noise Laminarization Nozzle-wall boundary layers	Unclassified – Unlimited

19. Security Classif. (of this report)	20. Security Classif. (of this page)	21. No. of Pages	22. Price*
Unclassified	Unclassified	57	Domestic, $3.50 Foreign, $6.00

*For sale by the National Technical Information Service, Springfield, Virginia 22151

CONTROL OF SUPERSONIC WIND-TUNNEL NOISE BY LAMINARIZATION OF NOZZLE-WALL BOUNDARY LAYERS

By Ivan E. Beckwith, William D. Harvey, Julius E. Harris,
and Barbara B. Holley
Langley Research Center

SUMMARY

Recent studies have shown that transition in hypersonic wind tunnels on simple bodies at small angles of attack is dominated by sound radiated from the turbulent boundary layers on the nozzle sidewalls. Therefore, one of the principal design requirements for a "quiet" tunnel, where realistic disturbance levels can hopefully be simulated, is to maintain laminar boundary layers on the nozzle walls at sufficiently high Reynolds numbers to obtain transition on test models.

An analysis of available information from previous investigations of six nozzles with exit Mach numbers from 2 to 20 indicates that laminar boundary layers are generally observed when values of the momentum thickness Reynolds numbers are less than 1500 and an acceleration parameter is greater than 4×10^{-7} over most of the supersonic part of the nozzle. Preliminary test results from a small rapid-expansion nozzle indicated that the use of high levels of acceleration in the subsonic approach did not significantly increase the operating pressure for which a laminar boundary layer could be maintained on the walls. Other factors such as the use of good design practices to obtain low turbulence and noise levels in the settling chamber and minimum wall roughness or disturbances with continuous wall curvature in the nozzle are probably more important than high acceleration. It is concluded that a combination of suction slots upstream of the throat and moderate levels of acceleration in the supersonic part of the nozzle offer the most practical design approach to the problem of maintaining laminar boundary layers on the nozzle walls up to higher Reynolds numbers than previously obtained.

INTRODUCTION

Recent general reviews on stability and transition of high-speed boundary layers and shear layers by Morkovin (refs. 1 to 3), Mack (ref. 4), and Mack and Morkovin (ref. 5) have reemphasized the amazing complexity of these phenomena and the many apparent contradictions and discrepancies in transition results. After 50 years of research, transition is still one of the major unsolved problems in fluid mechanics, although important

advances have been made in recent years as detailed in the proceedings of the 1967 (ref. 6) and the 1971 working meetings held at San Bernardino, California. The remaining contradictions and inconsistencies in transition data cannot be resolved without careful and detailed measurements of disturbance levels and spectra under controlled conditions.

It is now an established fact that intense sound generated by the turbulent boundary layers on wind-tunnel sidewalls dominates transition on simple bodies at small angles of attack for Mach numbers of about 3 or greater (refs. 1 to 14). Further research on transition under these circumstances is of little value without simultaneous measurements of disturbances. Also, to obtain reliable extrapolations of wind-tunnel transition data to flight conditions, these disturbances must be systematically reduced to low levels. A wind tunnel designed to provide a test environment with controlled and reduced disturbances is therefore required. Measurements made by Laufer (ref. 7) and Kendall (reported in ref. 1, p. 55) in the 20-inch tunnel at the Jet Propulsion Laboratory (JPL) have shown that when the sidewall boundary layers are laminar, the stream disturbance levels are reduced by an order of magnitude. Therefore, an important design requirement for such a tunnel is to maintain laminar boundary layers on the nozzle sidewalls up to sufficiently high operating pressures to obtain transition on test models. Laminar boundary layers have been maintained at relatively low supply pressures in several nozzles by techniques such as the use of rapid expansion (refs. 15 to 17, for example) and by lateral and longitudinal suction slots. (See discussion in ref. 10 of work at National Bureau of Standards (NBS) by Klebanoff and Spangenberg.) However, these nozzles were too small or the supply pressures at which laminar boundary layers could be maintained have been too low to obtain natural transition on test models.

The purpose of this report is to review and qualitatively compare the various techniques that have been applied or proposed for the maintenance of laminar boundary layers on nozzle walls at high Reynolds numbers. Preliminary test results of a small rapid-expansion nozzle are presented that indicate the technique of relaminarization of an initially turbulent boundary layer by large accelerations may not significantly reduce disturbance levels in the test flow. This technique, as well as others, such as boundary-layer control by suction through porous walls, encounters severe difficulties associated with fabrication and high costs that limit their consideration in the formulation of practical design requirements for a quiet tunnel.

The maintenance of laminar boundary layers is also important in several technological applications, other than for quiet wind tunnels, such as rocket nozzles and turbine blades where resulting improvements in performance and reductions in heat transfer are significant. (See refs. 18 to 21, for example.) Another area of concern related to the maintenance of laminar boundary layers in supersonic nozzles is the effect of free-stream turbulence and sound on heat transfer, particularly in the stagnation region of blunt bodies.

This problem has been studied in great detail for low-speed flows (refs. 22 to 24, for example) where free-stream turbulence levels as small as 2 percent may cause a 50-percent increase in heating. Such effects, although of smaller magnitude, are known to be present in supersonic tunnels where the stream disturbance levels are dominated by sound radiated from the sidewall boundary layers. Lastly, the accurate design of supersonic nozzles used to generate highly uniform test flows depends on the prediction and control of the nozzle wall boundary layers including the location and behavior of transition.

SYMBOLS

A	stream tube area
a	speed of sound
e	hot-wire output, volts
G	geometric parameter, $\frac{p_o}{p_e}\left(\frac{a_*}{u_e}\right)^2 \frac{d(u_e/a_*)}{d(s/y_*)}$
H	total enthalpy
K	acceleration parameter, $\frac{\mu}{\rho u_e^2}\frac{du_e}{ds}$
L	nozzle length from throat to exit
l_∞	mixing length in outer part of boundary layer (ref. 53)
M	Mach number
n	distance normal to wall
Δn	height or thickness of stream tube
P_G	Görtler instability parameter, $\frac{u_e\theta}{\nu}\sqrt{\frac{\theta}{r_o}}$
p	pressure
R	Reynolds number per unit length
R_a	ratio of longitudinal radius of curvature at the throat to throat radius, r_c/y_*

$R_{e,\theta}$	local momentum thickness Reynolds number, $\rho_e u_e \theta / \mu_e$
$R_{e,x,t}$	local transition Reynolds number based on wetted length
R_{ref}	reference Reynolds number based on throat radius or half height, $\frac{\rho_o a_* y_*}{\mu_o}$
r	radius of axisymmetric stream tube
r_*	radius of stream tube at sonic point
r_c	longitudinal radius of curvature at physical minimum
r_o	longitudinal radius of curvature of nozzle wall
S	normalized distance along nozzle contour, s/y_*
s	distance along contour of nozzle
T	absolute temperature
u	velocity in streamwise direction
x	axial distance from throat of nozzle
y	radius or half-height of nozzle
y_*	radius or half-height at physical throat of nozzle
γ	ratio of specific heats
δ	boundary-layer thickness where $\frac{u}{u_e}$ or $\frac{H - H_w}{H_e - H_w} = 0.995$
θ	momentum thickness of boundary layer
θ_{max}	wall angle at inflection point in subsonic approach of nozzle
μ	viscosity coefficient
ν	kinematic viscosity, μ/ρ

ρ mass density

σ standard deviation from least-squares curve fit of transition data (ref. 10)

Subscripts:

aw adiabatic wall

d design

e local conditions at "edge" of boundary layer

m measured

max maximum value

o conditions in settling chamber

T thermal boundary layer

t pitot pressure or total temperature

u velocity boundary layer

w evaluated at wall

∞ free-stream conditions in test region or near exit of nozzle

* free-stream conditions at sonic throat of nozzle or at sonic point in stream tube

1 initial value

A tilde over a symbol denotes the root-mean-square value, whereas a bar over a symbol denotes a mean value.

TEST REYNOLDS NUMBERS REQUIRED FOR TRANSITION ON WIND-TUNNEL MODELS

Before proceeding with the discussion of factors that influence and modify transition behavior in nozzle-wall boundary layers, some guidelines are necessary for the minimum values of test Reynolds numbers required to obtain transition on models in wind

tunnels with low disturbance levels. Although measurements of free-stream disturbances with flight vehicle instrumentation are scarce (see ref. 25 where some data with small probes are included), enough is known about atmospheric turbulence to indicate that the scales of disturbances are probably too large to affect transition at the higher altitudes where supersonic or hypersonic flight is of interest. Comparisons of flight and wind-tunnel transition data tend to confirm this general observation and also provide values of minimum test Reynolds numbers needed to design a quiet test facility.

A typical correlation of flight transition data on sharp cones at small angles of attack is compared with a correlation of corresponding wind-tunnel data (the wind-tunnel data points are not shown) in figure 1. The data and least-squares correlation methods are the same as those of reference 10. Comparison of the two correlations shows that for $2 < M_e < 8$, the wind-tunnel data correlation is smaller than the flight data correlation by almost an order of magnitude. The smaller values of $R_{e,x,t}$ for the wind-tunnel data are presumably due to the effects of wind-tunnel disturbances. Thus, from the flight data in figure 1, length Reynolds numbers up to about 20×10^6 will be required to obtain transition on test models if low disturbance levels approaching those of flight can be achieved in wind tunnels.

REVIEW OF RELAMINARIZATION IN LOW-SPEED FLOWS

The term "relaminarization" will be used throughout this report to denote the process whereby a boundary layer which is known to be turbulent at some upstream location reverts to a laminar or laminarlike boundary layer at some downstream station. This process can apparently occur as a result of large accelerations and/or large decreases in local density and the corresponding decreases in local Reynolds number. On the other hand, the term "laminarization" is used herein to describe the process that establishes a laminar boundary layer over some part of a test flow under conditions where no direct experimental knowledge of the upstream history of the boundary layer is available. Thus, for example, the wall boundary layer in the supersonic portion of a nozzle can be laminarized by reducing the supply pressure. Whether the boundary layers in the settling chamber and subsonic approach are also laminarized is not usually known.

Relaminarization of a turbulent boundary layer due to large acceleration was first observed in supersonic flow by Sternberg (ref. 26). However, most of the detailed data for both mean and fluctuating velocities in relaminarizing boundary layers have been obtained in low-speed flows (refs. 27 to 30, for example). Launder and Jones stated in reference 31 (see also ref. 32 by the same authors) that under a "severe" acceleration, "a complete degeneration to laminar flow will take place if the acceleration continues over a sufficient distance." This type of behavior of the mean velocity profiles and the normalized fluctuating velocities is observed when the acceleration parameter K exceeds

about 3×10^{-6} and the momentum thickness Reynolds number is simultaneously less than about 2000. However, in order for relaminarization to be a viable technique for a quiet tunnel, the residual turbulence in the relaminarized boundary layer must be very small since the sources of the free-stream sound disturbances are clearly the convected turbulent eddies in the supersonic boundary-layer flow. (See refs. 7 to 9, 33, and 34.) Measurements of turbulent velocity correlations including the Reynolds stress have been obtained in low-speed relaminarizing boundary layers. (See refs. 35 and 36.) When the Reynolds stress is normalized by the local free-stream velocity, the resulting ratio decreases significantly in the wall region of an accelerating flow.

Blackwelder and Kovasznay (ref. 36) have shown, however, that the decreases in this ratio are due mainly to the increase in the stream velocity and that the absolute levels of Reynolds stress may actually increase in the outer part of the boundary layer even when it is subjected to accelerations where $K > 4 \times 10^{-6}$. Although the overall history of the acceleration and the levels of Reynolds number (initial value of $R_{e,\theta}$ was 2500) are obviously involved, the results of this experiment imply that relaminarization by large accelerations may not always have the effect of reducing noise radiation in a supersonic boundary layer.

Laminar boundary layers have been observed on the walls of several supersonic nozzles and corresponding reductions in stream disturbance levels have been measured in at least three of these nozzles. Some of the factors apparently responsible for these observed laminar boundary layers will be considered in the next section.

LAMINAR BOUNDARY LAYERS IN SUPERSONIC NOZZLES

Laminarization has been reviewed briefly by Morkovin in the 1971 working conference at San Bernardino, California. He mentioned four wind-tunnel nozzles where laminar wall boundary layers have been observed. These nozzles and wind tunnels are described briefly in references 37, 38, 7 (the JPL 20-inch tunnel), and 8 (the Langley 22-inch helium tunnel). The question of whether relaminarization of an initially turbulent boundary layer actually occurred in these and other nozzles will be considered herein. An alternate explanation may be simply that the Reynolds number/or stream turbulence levels were low enough to maintain laminar boundary layers throughout the settling chamber, the subsonic approach, and the supersonic part of the nozzles. Obviously, the magnitudes of some characteristic Reynolds number and acceleration parameter are involved, as well as other factors such as wall roughness and curvature, flow disturbances in the upstream piping and valves, and disturbances in the settling chamber.

Observed Effects of Acceleration and Reynolds Number

Acceleration parameters.- In order to assess the possibility of obtaining laminar flow in nozzles at higher pressures by increasing the magnitude of K, the variations of

K_e and K_w with s/y_* are shown in figure 2 for several nozzles. (Methods for increasing K by modifications of geometry or other factors are considered later). These nozzles were selected for consideration herein because laminar boundary layers on the walls were observed over most of the supersonic part of the nozzles up to the stagnation pressures listed in the figure. As the stagnation pressure was increased a few percent above the listed values, transition either moved well up into the nozzles or fully turbulent flow was observed in all cases except the 4-inch Mach 5 nozzle. In this latter nozzle, recent unpublished results indicate that laminar flow could be maintained at somewhat higher stagnation pressures by heating the nozzle wall.

The distributions of K_e are shown in figure 2(a) for five nozzles. These nozzles are described in the references with the exception of the rapid-expansion nozzle of the Langley Research Center which will be described in more detail herein. The coordinates and Mach number distributions used to calculate the values of K are given in table I. It is seen that the limiting values of the laminarization parameter mentioned previously of $K = 2$ or 3×10^{-6} required to obtain laminarlike boundary layers in low-speed flows are exceeded in the subsonic approach region $\left(s/y_* < 10\right)$ in all cases except that of the JPL 20-inch tunnel. Nevertheless, laminar boundary layers and correspondingly low disturbance levels are obtained in the JPL tunnel up to a unit Reynolds number of about 0.6×10^6 per foot for $M_\infty = 4.5$. The maximum length Reynolds number on a flat plate in the test section at these conditions was about 3.3×10^6 for which the plate boundary layer was still laminar. (For further details of conditions for quiet operation of the JPL tunnel, see ref. 1 (p. 55).) Since the maximum values of K_e (fig. 2(a)) for the JPL tunnel are always below the "critical" levels of 2×10^{-6} or 3×10^{-6}, the observed laminar boundary layers on the nozzle wall in this case are probably due to other factors to be considered in more detail later. Some of these factors are the low Reynolds numbers, the excellent design of the settling chamber which was 1.24 m (8 ft) in diameter and had a turbulence level of 0.5 percent for $M_\infty < 4.5$, and the nozzle design which incorporates flexible walls with continuous third derivatives. (See ref. 7).

The other nozzles included in figure 2(a) all have values of K_e larger than the critical levels for laminarization in at least part of the subsonic approach. Thus, although no direct measurements are available, the boundary layers in these nozzles could presumably be relaminarized before entering the throat as reported previously in references 15 and 16 for conical nozzles. However, the critical levels of K_e are not maintained in the supersonic part of these nozzles; therefore, the laminar boundary layers observed there were probably not caused by large acceleration, or K_e is not the proper characteristic parameter.

Nash-Webber and Oates have suggested (ref. 17) that the relaminarization parameter should be based on gas properties evaluated at the wall for application to compressible flow. Accordingly, they defined and used the parameter

$$K_w = \frac{\mu_w}{\rho_w u_e^2} \frac{du_e}{ds} = \frac{\mu_w T_w}{\mu_e T_e} K_e \approx \left(\frac{T_w}{T_e}\right)^2 K_e \qquad (1)$$

The distributions of K_w for the same nozzles of figure 2(a) are shown in figure 2(b). Also included in figure 2(b) are the variations of K_w for nozzle A from reference 39 at two stagnation pressures. This is the only nozzle of those included in figure 2(b) where test data (ref. 39) showed that the boundary layer was turbulent upstream of the approach. (Data in this region are not available for the other nozzles.) Theoretical calculations for this case by the transition prediction procedure of McDonald and Fish (ref. 21) were in good agreement with the data.

Comparison of figure 2(b) with figure 2(a) shows that K_w is more nearly constant than K_e in the supersonic part of the nozzles. Also, K_w is greater than 4×10^{-7} over more than half the supersonic part of the nozzles. These larger values of K_w as compared with K_e are due to the small values of T_e caused by the large free-stream expansion of supersonic flow. From equation (1), K_w can also be increased by increasing T_w, and laminar flow at higher stream Reynolds numbers might then be expected. Recent unpublished results indicate that the wall boundary layer in the 4-inch Mach 5 nozzle was maintained laminar up to higher stagnation pressures by heating the nozzle wall. Whether this result can be attributed to the increase in K_w or to some effective reduction in roughness height relative to the increased boundary-layer thickness due to heating is not yet known. In general, heating the wall would tend to destabilize a laminar boundary layer so that increasing T_w may not always have the desired effect of maintaining laminar boundary layers for larger supply pressures.

The approximate locations and values of K_w for transition in nozzles 2, 4, and 5 are indicated in figure 2(b). Laminar flow was maintained to the exit for nozzles 1 and 3 at small values of K_w. The maintenance of laminar flow at larger values of Mach number in the supersonic part of these nozzles is therefore not dependent on large values of K_w.

Momentum thickness Reynolds number.- The next factors to be considered in evaluating the causes of laminar flow in these nozzles are the level and distribution of $R_{e,\theta}$ shown in figure 3 for the same nozzles of figure 2(a). These values of $R_{e,\theta}$ were computed for laminar flow by the finite-difference method of Harris (ref. 40) by using the coordinates and Mach number distributions listed in table I. Also shown in figure 3 are the variations of $R_{e,\theta}$ for a Mach 5 slotted nozzle at two values of stagnation pressure. This nozzle has an axisymmetric slot located upstream of the throat and the distributions of $R_{e,\theta}$ are shown downstream of the slot. The design and purpose of this nozzle will be discussed in more detail later in the report, but it is noted that even for

p_o = 138 N/cm^2 (200 psia), the maximum value of $R_{e,\theta}$ is about the same as in the JPL tunnel where laminar flow was obtained all the way to the nozzle exit at p_o = 5.3 N/cm^2 (7.7 psia). The values of $R_{e,\theta}$ upstream of the throat for all the nozzles vary from 20 to 1500. Downstream of the throat, the values of $R_{e,\theta}$ are generally less than 1000 except for the JPL tunnel where $R_{e,\theta}$ is nearly 2000 at the nozzle exit.

The maximum local value of $R_{e,\theta}$ for laminar flow is usually considered to be a reliable index for the occurrence of transition in a pressure gradient. (See ref. 41, for example.) The distributions of $R_{e,\theta}$ for nozzles 1 and 3 (fig. 3) indicate that laminar flow can be maintained for $R_{e,\theta} < 1500$ in the throat region and for $R_{e,\theta} < 2000$ near the nozzle exit. Laminar flow at these high values of $R_{e,\theta}$ cannot be obtained without extremely low levels of both mean and fluctuating disturbances in the free stream throughout the nozzle and settling chamber. From known design requirements for these nozzles (refs. 7 and 37), other factors of equal importance are smooth walls with no steps or discontinuities and continuous second and third derivatives along the nozzle walls. Also, recent unpublished data obtained in the 4-inch Mach 5 nozzle indicate that "natural" deposits of dust and dirt in the throat region of a nozzle may reduce the transition Reynolds numbers for nozzle-wall boundary layers by a factor of two.

History of acceleration and Reynolds number.- Nash-Webber and Oates (ref. 17) introduced the concept of the "trajectory" of a boundary layer in the $K_w, R_{e,\theta}$ plane to describe the history of boundary layers in a rapidly expanding flow. They showed that an initially turbulent boundary layer would be completely or partially relaminarized depending on how far a critical region of the $K_w, R_{e,\theta}$ plane is penetrated by the trajectory.

Figure 4(a) is a plot of K_w against $R_{e,\theta}$ for data from several investigations including low-velocity incompressible channel flows (refs. 27 to 30, 42, and 43), the approach and transonic region of nozzles (refs. 16, 17, 44, 45, and 46), and supersonic wind-tunnel nozzles with exit Mach numbers from 4.6 to 20 (refs. 7, 8, 37, and 11). (The Langley rapid-expansion and slotted nozzles will be described in a subsequent section.) Figure 4(b) gives the symbol key, the type of apparatus, and other comments for the data shown in figure 4(a). Note that line symbols are used for all supersonic and hypersonic wind-tunnel nozzles. These cases are the same as those used in figures 2 and 3. The extent of laminar boundary layers in these nozzles is also indicated in the key to the figure. The slotted nozzle is designed to maintain a laminar boundary layer up to p_o = 138 N/cm^2 (200 psia); however, data from this new nozzle are not yet available. The open symbols in the figure represent data where heat-transfer or boundary-layer profile data indicated that partial or complete relaminarization had occurred. All these data are above the Nash-Webber – Oates criteria. The earlier criteria of Launder (ref. 27) and Kline, et al (ref. 29) are also shown and would apply equally well to the data points

shown in the figure. The starting point of trajectories for the nozzles that started or ended within the critical Nash-Webber – Oates region are marked with an asterisk. The starting point for the remaining nozzle trajectories are marked with an X. As would be expected from the results in figure 2, the trajectory for the JPL tunnel is always outside the region where relaminarization of initially turbulent boundary layers has been observed. It may therefore be concluded that the laminar boundary layer observed on the walls of the JPL tunnel at the conditions shown in figures 2 to 4 was not caused directly by acceleration but rather by the favorable design features of the settling chamber and nozzle coupled with the low Reynolds numbers in the approach and throat regions.

Comparison of the trajectories in figure 4 for the supersonic and hypersonic wind-tunnel nozzles (line symbols) with the data for turbulent boundary layers (closed symbols) indicates that supersonic nozzle-wall boundary layers can be maintained laminar at much lower levels of K_w than is possible in low-speed channel flows or in subsonic approach regions of nozzles. Hence, the trajectory for the slotted nozzle at the higher pressure (case 6a) indicates that laminar flow might be expected at this pressure of 138 N/cm^2 (200 psia) since the values of $R_{e,\theta}$ are generally less than those for cases 1 and 3 which had laminar flow to the nozzle exits.

Reference Reynolds numbers based on throat size.- The values of a reference Reynolds number R_{ref} based on throat radius or half-height for several nozzles including those in figures 2 and 3 are given in table II. Values of the free-stream unit Reynolds numbers at the exit Mach number M_∞ are also listed. Values of y_*, p_0, and T_0 are included in table II as are comments on the observed boundary-layer behavior at the stations noted. Comparison of these values of R_{ref} shows that the JPL tunnel has the lowest values of R_{ref}, whereas the Langley 4-inch Mach 5 and rapid-expansion nozzles have the largest values. As noted previously, laminar flow was not maintained all the way to the exit in these two latter nozzles. The extent of laminar flow in the supersonic part of the Nash-Webber nozzle and the JPL conical nozzles is not known; therefore the large values of $R_{ref} \approx 4 \times 10^{-5}$ for these nozzles cannot be taken as an index of laminar flow in the entire nozzle. Hence, the value of R_{ref} is not an exclusive or reliable index for laminar or transitional boundary layers in supersonic nozzles. Rather, the values of R_{ref} at which laminar flow was maintained or for which laminarization occurred depend on various factors such as the flow acceleration and the nozzle length. Thus the "critical" values of R_{ref} for relaminarization in the subsonic approach increase as K increases, as shown by the results for the JPL conical nozzles (ref. 16). Also, as the nozzle lengths are increased, the values of R_{ref} for which laminar flow could be maintained to the nozzle exit are generally decreased as indicated by the comments in table II.

The values of unit Reynolds numbers at the nozzle exits together with the physical size of the nozzles provide a rough guide for the maximum test Reynolds numbers that

could be obtained on models in these tunnels under "quiet" conditions. (Note, however, that the Nash-Webber nozzle and the JPL conical nozzles were not designed and tested as wind-tunnel facility nozzles.) Thus, the large values of R_∞ for the Langley 4-inch Mach 5 nozzle would provide a maximum length Reynolds number of about 5×10^6 which is not large enough to obtain transition on the model if the maximum levels of transition Reynolds numbers observed in flight (see fig. 1) are to be achieved. As mentioned previously, the smaller values of R_∞ in the JPL 20-inch tunnel gave a maximum length Reynolds number of about 3.3×10^6 which was too small to obtain transition on a flat-plate model.

Rapid-Expansion Nozzles

Review of the data (refs. 16, 17, 45, and 46) in the preceding sections of this report has shown that when $K_e > 2 \times 10^{-6}$ or 3×10^{-6} and $R_{e,\theta} < 1500$ in the subsonic approach region of nozzles, the initially turbulent boundary layer appears to become laminar. This relaminarization phenomenon has been evidenced primarily in the mean velocity profiles and surface heating rates although some investigations have indicated that the turbulent fluctuations may not be completely damped until K_e is maintained at higher levels for long distances. On the other hand, laminar boundary layers have been maintained in the supersonic parts of several nozzles if $K_w > 4 \times 10^{-7}$ downstream of the throat. Hence, it is desirable to determine whether K_w can be increased by modifications to the geometry of the nozzle. Thus, by noting that $p_w = p_e$, equation (1) may be written as

$$K_w = \frac{\mu_w T_w}{\mu_o T_o} \frac{G}{R_{ref}} \tag{2}$$

where $G = \frac{p_o}{p_e}\left(\frac{a_*}{u_e}\right)^2 \frac{d\left(u_e/a_*\right)}{d\left(s/y_*\right)}$ which is determined entirely by the geometric shape of the nozzle. Of course, for a given shaped nozzle, K_w may be increased by reducing R_{ref} or by increasing T_w. However, one of the main requirements for a quiet tunnel is to maintain laminar boundary layers on the walls at larger Reynolds numbers; therefore, R_{ref} must be as large as possible. As mentioned previously, recent unpublished data obtained in the 4-inch Mach 5 nozzle indicated that laminar wall boundary layers were maintained at higher pressures by heating the nozzle wall. This effect may be due to the larger values of K_w; however, increasing T_w would also destabilize the boundary layer. Thus these two effects would be in opposition. The geometric parameter G can be increased in the throat region of a nozzle by increasing the wall angle of the subsonic approach and by decreasing the longitudinal radius of curvature in the throat.

Langley 4-inch rapid-expansion nozzle.- In order to test the possibility of obtaining laminar flow in nozzles at higher Reynolds numbers by increasing G, the method of reference 47 has been used to design the transonic part of a nozzle with large values of acceleration in the approach region and in the throat. In the notation of reference 47, the parameters R_a and θ_a designate the nominal throat radius of curvature and the maximum wall angle in the approach, respectively. The values chosen for the first test nozzle were $R_a = 0.25$ and $\theta_a = 75^o$. The supersonic part of this nozzle was designed by an inverse method of characteristics similar to that of reference 48 but with the center-line distribution faired to match the distribution from the transonic series solution (ref. 47). A small part of the nozzle contour just downstream of the minimum was not computed directly by this inverse method; therefore, the accuracy of the final faired nozzle coordinates was checked by calculating the flow field with a direct method of characteristics. (See ref. 49.) The faired coordinates and the supersonic flow across the nozzle just downstream of the minimum were used as inputs for this calculation.

The Mach number distribution along the center line of this nozzle computed by the direct method of characteristics is plotted in figure 5 which shows large disturbances along the center line. However, the calculated flow distribution along the wall was smooth and monotonic; therefore, the design was considered to be satisfactory for the present purpose of assessing the effect of large accelerations on the nozzle-wall boundary layer. (The nozzle was not designed to provide a uniform test flow at the exit.) The two sets of experimental data shown in the figure were obtained from pitot pressure measurements and by assuming isentropic expansion from the measured settling chamber pressure. The data for the original machined nozzle are in reasonable agreement with the calculation except for $x < 5$ cm (2 in.). Subsequent measurements of the nozzle coordinates showed large discrepancies from the design coordinates as shown in figure 6 which is a plot of the differences between the design and measured coordinates. The nozzle was then remachined and the resulting coordinates were in better agreement with design values as shown in figure 6. However, the surface was somewhat rough and wavy. The experimental data for the center-line Mach number distribution (fig. 5) after remachining the nozzle are in better agreement with the calculation (using the design coordinates). This result indicates that the combination of the Hopkins-Hill transonic solution (ref. 47) with the direct method of characteristics (ref. 49) gives a satisfactory prediction of inviscid nozzle flow for small throat radii of curvature.

The effect of the rapid expansion on the distributions of K and $R_{e,\theta}$ has been presented for this nozzle in figures 2 to 4. The behavior of the nozzle-wall boundary layer was determined indirectly from measurements of fluctuating pitot pressure at the nozzle exit by the same instrumentation and methods described in reference 11. The results for the original machined nozzle are shown in figure 7. The peak values of $\tilde{p}_t/\bar{p}_t$ are associated with the peak in transitional disturbances in the nozzle-wall boundary layer

(see appendix) and therefore correspond to the "end" of transition at its "acoustic origin" with respect to the probe location. The term "acoustic origin" was coined in reference 8 and refers to the nearest upstream location in the nozzle-wall boundary layer from which radiated sound can impinge on a sensing instrument in the test flow. Thus for the particular settling chamber screen configuration (No. 3 as described in ref. 11) used for these tests, transition occurred 10.2 to 15.2 cm (4 to 6 in.) upstream of the nozzle exit at $p_o \approx 34.5$ N/cm^2 (50 psia) for the conventional Mach 5 nozzle and at $p_o \approx 41.4$ to 62 N/cm^2 (60 to 90 psia) for the rapid-expansion nozzle. The level of $\tilde{p}_t/\bar{p}_t$ is lower for the rapid-expansion nozzle possibly because of the smaller volume of turbulent boundary layer in this nozzle due to the shorter length of the nozzle and the larger favorable pressure gradients compared with those of the conventional nozzle. (See ref. 50.) The larger favorable pressure gradients in the rapid-expansion nozzle may also tend to reduce the turbulent shear and thereby the intensity of the radiated sound. Thus, the increased acceleration may have delayed transition to a slightly higher stagnation pressure (and therefore a higher value of R_{ref}) but otherwise had little effect on stream disturbance levels. Further tests will be required to determine whether this relatively small effect of the large acceleration (and resulting large values of K) in the approach region on the nozzle-wall boundary-layer transition was caused by the machining errors (fig. 6) and wall waviness, nonuniformities in the inviscid flow (fig. 5), the persistence of residual turbulence (as in ref. 36), or the smaller values of K_e and K_w in the supersonic part of the nozzle (fig. 2).

Design of nozzles for specified values or distributions of K.- As part of a general study of relaminarization in nozzle-wall boundary layers, it is necessary to determine the general requirements for nozzle geometry to give a constant value of K or a specified K distribution. The resulting nozzle shapes would have to be consistent with the requirement of a uniform test flow, if the technique of relaminarization is to be useful for wind-tunnel facilities. Thus, consider the one-dimensional annular stream tube in the inviscid flow near the wall of an axisymmetric nozzle as illustrated in sketch (a).

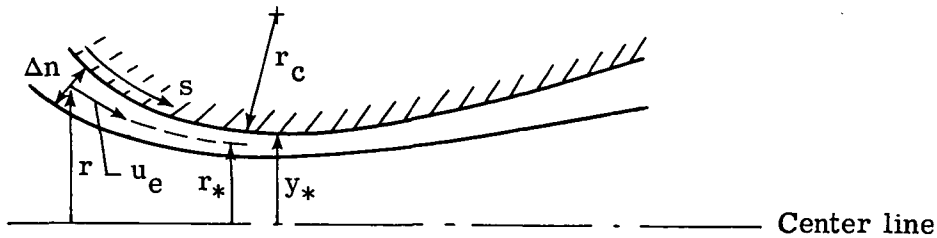

Sketch (a)

Continuity requires that

$$\frac{\rho_e}{\rho_*}\frac{u_e}{a_*}\frac{A}{A_*} = 1.0 \tag{3}$$

where, in general, $A = 2\pi r\,\Delta n$. For isentropic flow of an ideal gas with constant specific heats and by the use of the adiabatic energy equation, the continuity equation may be written as

$$\left(\frac{p_e}{p_*}\right)^{1/\gamma}\left[\frac{\gamma+1}{\gamma-1}-\frac{2}{\gamma-1}\left(\frac{p_e}{p_*}\right)^{\frac{\gamma-1}{\gamma}}\right]^{1/2}\qquad\frac{A}{A_*}=1.0 \tag{4}$$

For the same conditions, and again by the use of the adiabatic energy equation, the acceleration parameter K_w may be written from equation (2) as

$$K_w=-\frac{1}{\gamma}\left(\frac{\gamma+1}{2}\right)^{\frac{\gamma}{\gamma-1}}\frac{\mu_w T_w}{\mu_o T_o}\frac{1}{R_{ref}}\frac{\frac{d}{dS}\left(p_e/p_*\right)}{\left(\frac{p_e}{p_*}\right)^{\frac{1+\gamma}{\gamma}}\left[\frac{\gamma+1}{\gamma-1}-\frac{2}{\gamma-1}\left(\frac{p_e}{p_*}\right)^{\frac{\gamma-1}{\gamma}}\right]^{3/2}} \tag{5}$$

Numerical integration of this equation establishes the relation between p_e/p_* and S for any desired variation of T_w and K_w with S. Equation (4) then gives the corresponding area ratio variation along the stream tube.

As a simple example of this procedure, T_w and K_w are specified as constants, and equation (5) then gives

$$S-S_1=-\frac{1}{\gamma}\left(\frac{\gamma+1}{2}\right)\frac{\mu_w T_w}{\mu_o T_o}\frac{1}{K_w R_{ref}}\int_{(p_e/p_*)_1}^{p_e/p_*}\frac{d\left(p_e/p_*\right)}{\left(\frac{p_e}{p_*}\right)^{\frac{1+\gamma}{\gamma}}\left[\frac{\gamma+1}{\gamma-1}-\frac{2}{\gamma-1}\left(\frac{p_e}{p_*}\right)^{\frac{\gamma-1}{\gamma}}\right]^{3/2}} \tag{6}$$

Then if one-dimensional flow is assumed

$$\frac{A}{A_*}=\left(\frac{r_w}{y_*}\right)^2$$

and the corresponding nozzle shape can be easily computed from equation (4). Results of this computation for two values each of R_{ref} and T_w and with $M_\infty = 5.0$ are shown in figure 8. It is seen that for the smaller value of $R_{ref} = 5 \times 10^5$, realistic nozzle shapes are obtained, especially for $T_w = 467$ K (840° R). This value of R_{ref} corresponds to conditions for which laminar flow to within about 10 cm (4 in.) of the nozzle exit was observed in both Langley Mach 5 nozzles. (See appendix and table II.) For the larger value of R_{ref}, the supersonic portions of the nozzles are not realistic for use as wind-tunnel nozzles where uniform flow must be obtained at the nozzle exit. The nozzle shapes for the subsonic approach regions are satisfactory as indicated by comparison with the Hopkins-Hill transonic solution (ref. 47) for $R_a = 0.5$ and $\theta_{max} = 45°$. Figure 9 shows how these parameters vary with R_{ref} and T_w for $K_w = 2 \times 10^{-6}$. Large values of R_{ref} cannot be obtained without small values of R_a and large values of θ_{max}. Since $K_w = 2 \times 10^{-6}$ is probably not large enough to achieve complete laminarization (see previous discussion) and since larger values of K_w would require even shorter nozzles with larger values of θ_{max} and smaller values of R_a, it must be concluded that laminarization of nozzle-wall boundary layers by large acceleration, particularly in the supersonic portion of the nozzle, is not practical. Furthermore, accurate machining of this type of nozzle is difficult (fig. 6) and large values of θ_{max} lead to flow separation problems upstream of the subsonic approach.

PROPOSED TECHNIQUES AND GENERAL REQUIREMENTS FOR LAMINAR FLOW NOZZLES

In an early review of methods for minimizing free-stream disturbances in supersonic wind tunnels, Morkovin (ref. 50) was concerned mainly with the problem of reducing the intensity of sound radiation from turbulent boundary layers since at that time there was little hope of maintaining laminar boundary layers at high Reynolds numbers. Since that time, Klebanoff and Spangenberg at NBS have been able to maintain laminar boundary layers on the walls of a small Mach 2 nozzle up to a length Reynolds number of 3.3×10^6 by suction through a combination of lateral scoops upstream of the throat and longitudinal slots downstream of the throat. (A brief discussion of this work at NBS is included in ref. 10.)

Design of Slotted Laminar Flow Nozzles

In view of the limited possibilities and difficulties of obtaining laminar boundary layers on nozzle walls by using large accelerations, the use of lateral scoops to remove the turbulent boundary layer upstream of the throat, as in the NBS tests, seems to be worthy of further investigation. The use of lateral suction slots in supersonic flow will also maintain laminar boundary layers to higher Reynolds numbers but at the expense of

introducing steady disturbances into the free-stream. (See ref. 51.) Steady disturbances of this type would be expected to degrade transition data considerably; therefore, removal of the boundary layer just upstream of the throat appears to be attractive for the nozzle of a quiet tunnel.

Figure 10 is a sketch of a typical design for a slotted throat. In this case the transonic region was computed by the method of reference 47 for $R_a = 0.5$ and $\theta_{max} = 45^o$. The supersonic region was computed by the method of characteristics by using as inputs the flow conditions just downstream of the sonic line from the Hopkins-Hill transonic solution and a faired velocity distribution along the center line. Some of the streamlines and constant Mach number lines in the transonic region are shown in the figure. The Langley Mach 5 slotted nozzle was designed by this method but the Hopkins-Hill parameters chosen were $R_a = 1.0$ and $\theta_{max} = 45^o$. The larger radius of curvature was used to alleviate fabrication difficulties in the throat region while maintaining sufficient acceleration to stabilize the laminar boundary layer at higher operating pressures. Fabrication of this new slotted nozzle is now completed. Comparisons of $R_{e,\theta}$ and K_w distributions (downstream of the slot) for this nozzle with previous results in figures 3 and 4 indicated that laminar flow up to $p_o = 138$ N/cm^2 (200 psia) may be possible. The value of R_{ref} at this pressure is 2.6×10^6 which is three times larger than the highest value recorded for laminar or transitional flow in nozzles. (See table II.)

The slot height for this type of nozzle must be large enough to pass the entire turbulent boundary layer from the settling chamber and subsonic approach including any intermittent bursts. The thermal boundary layer must also be considered since it may be thicker than the velocity boundary layer in the favorable pressure gradient region. (See refs. 15 and 44.) Predicted values of several boundary-layer parameters in the subsonic approach of the Langley Mach 5 slotted nozzle (for $R_a = 1.0$, $\theta_{max} = 45^o$) are shown in figure 11. The methods of references 40 and 52 have been used to compute δ_u, δ_T, and θ for fully turbulent flow at $p_o = 103.5$ N/cm^2 (150 psia). A constant value of the dimensionless mixing length $l_\infty/\delta_u = 0.09$ was used in these calculations and the boundary-layer thickness at 1.52 m (5 ft) (x = -0.583 m (-1.912 ft)) downstream from the last settling chamber screen was taken as $\delta_{u,o} = 0.0158$ m (0.052 ft). The method of reference 53 was used to calculate δ_u, θ, and the normalized mixing length l_∞/δ_u for $p_o = 103.5$ N/cm^2 (150 psia) and for two settling chamber turbulence levels $(\tilde{u}/u_e)_o = 0.01$ and 0.06. The mixing length is obtained in the method of reference 53 from an integral form of the turbulence kinetic energy equation and hence is an index of the magnitude of the Reynolds stress and turbulence intensity in the outer part of the boundary layer. Comparisons of predictions by this method with experimental data in references 21 and 53 have shown that when free-stream disturbance effects can be characterized in terms of root-mean-square (rms) levels, the method is able to predict reliably the transition from laminar to turbulent flow for both subsonic and supersonic speeds and retransition (or relam-

inarization) from turbulent to laminar flow for subsonic speeds. The results shown in figure 11 from the method of reference 53 have been supplied to NASA by United Aircraft Corp. (Contract NAS 1-11917).

Comparisons of δ_u and δ_T from the methods of references 40 and 52 (figs. 11(a) and 11(b)) show that $\delta_T > \delta_u$ in the region of large pressure gradient near the slot lip. The height of the slot lip (fig. 11(b)) was determined from the preliminary design and boundary-layer calculations for the nozzle so that the entire boundary layer would be removed by the slot plus some of the nominal inviscid flow to allow for intermittent turbulent bursts. Results of the final boundary-layer calculations using an adjusted and smoothed u_e distribution indicate that for the original design location of the slot lip, the outer intermittent edge of the thermal boundary layer may not be removed by the slot. (See fig. 11(b).) Upstream translation of the slot lip with respect to the approach is provided for in the design and should correct this situation. Results shown in figure 11(d) indicate that the boundary layer in the subsonic approach may be laminarized before it reaches the slot even at $p_o = 103.5$ N/cm^2 (150 psia). The boundary-layer thickness may be reduced by laminarization according to calculations for δ_u by the method of reference 53 shown in figure 11(a). The purpose of the slot is to remove all residual turbulence and settling chamber vorticity remaining in the boundary layer at the lip of the slot where $M_e \approx 0.34$. Comparisons of δ_u and θ, from the methods of references 40 and 52 (wherein completely turbulent flow was assumed), with corresponding results from reference 53 indicate some disagreement especially in the region where $M_e < 0.1$. These large values of δ_u and θ predicted for this region by the method of reference 53 are believed to be due to the larger values of δ_u and θ calculated in the settling chamber. Thus, the value of δ_u at $x = -0.58$ m (-1.912 ft) was 0.02 m (0.075 ft) or about 44 percent larger than the values used in the methods of references 40 and 52. It is also of interest that the smaller turbulence level of $\left(\tilde{u}/u_e\right)_o = 0.01$ results in predictions of smaller boundary-layer thicknesses and earlier laminarization. Calculations by the method of reference 53 also indicate that lower settling chamber turbulence levels would delay transition of the new laminar boundary layer downstream of the slot; however, this possibility must await experimental confirmation.

Importance of Minimizing Disturbances in Settling Chamber and Supply Air

The three types of free-stream disturbances that can exist in supersonic tunnels are fluctuations in vorticity (or turbulence $\tilde{u}/\overline{u}$), entropy $\left(\text{or total temperature } \tilde{T}_t/\overline{T}_t\right)$, and sound (or pressure $\tilde{p}/\overline{p}$). Both the longitudinal and lateral components of turbulence in the settling chamber are greatly reduced by the large expansion ratios for $M_\infty > 4$ (ref. 54). Morkovin has stated (ref. 50) that "a relatively high turbulence level of 0.5 percent or less in the settling chamber should prove satisfactory even for measurements of transition in the supersonic section." However, in order to laminarize the wall boundary

layers (or to maintain laminar boundary layers), the results presented in the preceding section indicate that lower turbulence levels may be required. Results of Spangler and Wells (ref. 55) show that low-frequency acoustic disturbances must also be minimized to avoid premature transition in a low-speed boundary layer. It is therefore essential to eliminate any steps or discontinuities in the walls of the settling chamber and approach that could generate additional vorticity or sound.

Sources of low-frequency fluctuations sometimes observed in the free-stream and wall boundary layers of supersonic tunnels (refs. 56 and 57) can probably be traced to locally separated regions at the entrance or diffuser of the settling chamber or immediately downstream of high-density screens or filters. Test results in the Langley Mach 8 variable-density hypersonic tunnel presented by Stainback et al. in reference 14 show that transition Reynolds numbers on test cones were increased significantly by the addition of a high-density porous plate just downstream of the settling chamber entrance. In this case, the porous plate probably prevented or alleviated separation at the entrance cone of the settling chamber.

Another problem, mentioned in reference 58, is related to local instabilities (downstream of high-density filters, for example) that may generate aerodynamic sound which intensifies rapidly with increasing dynamic pressure. According to reference 58, undesirable resonant coupling with acoustic modes in the supply channel or elsewhere may then be set up. Stainback et al. (ref. 14) measured $\tilde{p}_w/\bar{p}_e$ on a 16° half-angle cone in the Langley Mach 8 variable-density hypersonic tunnel for different arrangements of upstream valves and piping. When all the supply air was routed through a 5-cm-diameter (2-in.) bypass pipe, the normalized root-mean-square sound level was increased by 50 percent at low operating pressures. Of course, this effect may not be caused by resonant coupling, but the results do indicate that sound generated in the settling chamber or upstream piping is convected into the hypersonic test flow. Morkovin had suggested earlier (ref. 50) that the intensity of sound propagated into the supersonic section of a tunnel from upstream sources may be insignificant because of "the choking effect of the sonic throat." In any case, it is obvious that the design requirements of the upstream piping and settling chamber are important for a quiet tunnel.

The arrangement of settling chamber "turbulent manipulators" (ref. 58) may also be critical in attempts to delay transition in tunnel-wall boundary layers. New results in reference 11 (see fig. 16 in ref. 11) have reemphasized this requirement which is often overlooked in the design of hypersonic facilities. Data in reference 11 showed that the use of different settling chamber components had large effects on the levels and distribution of $\tilde{p}_t/\bar{p}_t$. This ratio was nearly doubled, for example, when high-density porous plates were located downstream of more open screens. This result would be expected from previous investigations (refs. 58 and 59). More recent unpublished data in the same

Mach 5 tunnel indicate that these types of changes may not have a direct effect on nozzle-wall boundary-layer transition.

Effects of Normal Density Gradients and Wall Curvature on Stability of Supersonic Boundary Layers

Rotta (ref. 60) has shown that the density stratification in compressible boundary layers is stable on a concave wall when

$$\frac{\gamma - 1}{\gamma p}\frac{\partial p}{\partial n} - \frac{1}{T}\frac{\partial T}{\partial n} < 0$$

Sketch (b) illustrates qualitatively the pressure and temperature distributions in the boundary layer on the downstream concave wall of a supersonic nozzle:

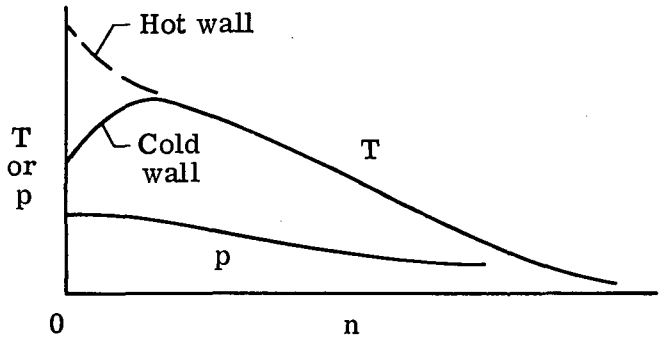

Sketch (b)

The pressure distribution is imposed by the expansion and Mach line "cancellation" processes in the local inviscid flow required to produce the uniform test flow in a nozzle. However, over most of the boundary layer $\left|\frac{1}{T}\frac{\partial T}{\partial n}\right| >> \left|\frac{\partial p}{p\,\partial n}\right|$; therefore, near a cold wall the density stratification is stable whereas farther from the wall the density stratification is unstable and favors the formation of longitudinal (Görtler or Taylor) vortices.

Kobayaski (ref. 61) has shown that homogeneous suction always increases the stability of an incompressible laminar boundary layer in regard to the formation of Görtler vortices. He has also suggested that the Görtler instability will predominate over Tollmien-Schlichting instability along a concave wall with suction so that the transition point will be determined by the former type of instability.

Görtler's instability parameter is defined as

$$P_G = \frac{u_e \theta}{\nu}\sqrt{\frac{\theta}{r_o}}$$

The theoretical minimum critical values of P_G range from about 0.4 up to 10 (for incompressible flow) depending on the lateral wavelength spacing of the vortices (ref. 61). Minimum critical values of P_G based on transition data in low-speed flows range from about 5 to 20 according to reference 62, or from the data of Liepmann (discussed in ref. 63) transition occurs when $P_G > 7$. Maximum values of P_G (corresponding to maximum instability) in the supersonic concave regions for nozzles with laminar boundary layers on the walls are as follows:

Nozzle	Facility	M_∞	p_o		$(P_{G,e})_{max}$
			N/cm^2	psia	
1	JPL 20-inch	4.6	5.3	7.7	12
2	Univ. of Michigan	8.0	68.9	90	7
3	4-inch LaRC	5.0	34.5	50	6
4	Rapid expansion	5.0	34.5	50	6.5

(For more information on these nozzles, see previous sections of this report and table II.) It is seen that the values of P_G for these nozzles are within the range of critical values mentioned above. For the listed conditions, transition did not occur in nozzles 1 and 2, but sometimes did occur in nozzle 3 (see appendix and ref. 12) and nozzle 4 a short distance upstream of the nozzle exits. Recent data obtained by the oil film technique indicate that Taylor-Görtler vortices began to form in the 4-inch LaRC nozzle at $p_o \approx 28$ N/cm^2 (40 psia), whereas transition to fully turbulent flow finally occurs at $p_o \approx 41$ N/cm^2 (60 psia). Thus, transition in these nozzles may have been caused by this instability. Observed deviations from predicted laminar profile shapes between the last two stations of nozzle 3 (see appendix) for $p_o = 34$ N/cm^2 (50 psia) may also have been caused by the effect of Görtler vortices on the laminar boundary layer.

The maximum values of P_G for the new Mach 5 laminar-flow slotted nozzle are 5.9 and 7.8 for $p_o = 34.4$ and 103 N/cm^2 (50 and 150 psia), respectively. Therefore, based on these results for nozzles 1, 2, and 3, transition due to Görtler instability may occur in the slotted nozzle at the higher pressure.

Porous Wall Suction

Previous tests at Langley indicated that transition Reynolds numbers on test models in a small Mach 4 nozzle were not increased by suction at the porous walls of the nozzle. The results were discussed briefly in reference 10. The failure to increase transition Reynolds numbers in these tests was probably due to poor control of suction flow rates, roughness effects, and hole suction effects, all of which could increase the free-stream disturbance levels.

Tests conducted by Klebanoff and Spangenberg at NBS (discussed in ref. 10) in which the porous wall (or area) suction concept was applied to the sidewall of a Mach 2 nozzle resulted in transition Reynolds numbers up to about 3×10^6. However, free-stream disturbances were detected that were apparently caused by nonuniform suction. The presence of these disturbances indicated that the porous material used for these tests would not be suitable for use in a quiet tunnel. Further tests with improved porous materials will be required to determine whether area suction will maintain laminar boundary layers at sufficiently high Reynolds numbers without causing unacceptable free-stream disturbances.

Calculations by W. Pfenninger and J. Syberg at Boeing Co. (Contract NASw-2359) indicate that the boundary layer on the wall of a Mach 8 nozzle with an exit diameter of 1 m (≈39 in.) can be completely stabilized with respect to both Tollmien-Schlichting and Görtler disturbances up to a unit Reynolds number of 26×10^6 per m (8×10^6 per ft) by the use of area suction. Thus, if the practical problems of cost, surface finish, and precise control and distribution of suction flow rates with acceptable free-stream disturbances can be solved, this technique would maintain laminar boundary layers up to useful values of test Reynolds numbers of 20×10^6 to 30×10^6 for a 1.2-m-long (4-ft) model.

CONCLUDING REMARKS

Free-stream disturbances in wind tunnels for Mach numbers greater than 3 are dominated by sound radiated from the turbulent boundary layers on the nozzle walls. Therefore, one of the important design requirements for a quiet supersonic or hypersonic tunnel is to maintain laminar boundary layers on the nozzle walls and thereby eliminate this source of free-stream disturbance.

Review of low-speed results indicates that the mean velocity profile shapes of initially turbulent boundary layers tend to approach those for laminar boundary layers when an acceleration parameter K exceeds about 3×10^{-6} and the momentum thickness Reynolds number $R_{e,\theta}$ is simultaneously less than about 2000. However, the absolute magnitude of the turbulent fluctuations may not decrease significantly until K is maintained at even larger values with smaller values of $R_{e,\theta}$ for long distances. Thus, upstream relaminarization by large accelerations may not reduce the turbulence intensity in the downstream supersonic boundary layer. No reduction in the noise radiated from supersonic boundary layers would then be expected. Tests of a small rapid-expansion nozzle, although not conclusive, tend to confirm that relaminarization of an initially turbulent boundary layer does not reduce sound radiation significantly. This problem and others associated with the rapid-expansion concept, such as machining tolerances, nozzle geometry, and possible flow separation in the subsonic approach, indicate that this relam-

inarization technique of maintaining large levels of $K > 2 \times 10^{-6}$ may not be desirable for quiet tunnel applications.

Analysis of available information on several nozzles with exit Mach numbers from 2 to 20 has indicated that laminar wall boundary layers are generally observed when $R_{e,\theta}$ is less than 1500 in the throat region and less than 2000 near the exit. Also, an acceleration parameter based on gas properties evaluated at the wall should apparently be greater than 4×10^{-7} over most of the supersonic part of the nozzle to maintain laminar wall boundary layers. Other factors of equal importance are low levels of vorticity and acoustic disturbances in the settling chamber, smooth walls with no steps or discontinuities throughout the settling chamber and nozzle, and continuous derivatives along the nozzle walls.

Another factor that can cause premature transition on the concave wall of a supersonic nozzle is the presence of Görtler instabilities which cause longitudinal vortices. Calculation of the maximum values of Görtler's instability parameter P_G for these nozzles with laminar and transitional boundary layers indicates a critical range for transition of $P_G \approx 6$ to 12. To maintain larger values of the acceleration parameter K, shorter nozzles are required with smaller radii of curvature which, in turn, increase P_G and the susceptibility of the boundary layer to the Görtler instability. However, this effect may be offset by the smaller values of momentum thickness in the shorter nozzles and by cooling the wall.

Calculations reported herein indicate that nozzle-wall boundary layers can be laminarized up to large Reynolds numbers by area suction. However, the practical problems of nozzle construction from porous materials would preclude this technique as a first choice.

Consideration of all these factors indicates that a combination of suction slots upstream of the throat and moderate acceleration in the supersonic region of the nozzle offers the most practical design approach to the problem of maintaining laminar boundary layers on nozzle walls up to sufficiently high Reynolds number to obtain transition on test models. Length Reynolds numbers of at least 20×10^6 will be required to obtain transition on test models in supersonic wind tunnels with low-stream-disturbance levels.

Langley Research Center,
National Aeronautics and Space Administration,
Hampton, Va., September 11, 1973.

APPENDIX

TRANSITIONAL CHARACTERISTICS OF THE BOUNDARY LAYER ON THE WALL OF A MACH 5 NOZZLE

By P. Calvin Stainback, William D. Harvey,
and John B. Anders
Langley Research Center

Tests have been conducted in a small Mach 5 nozzle (ref. 11) at the Langley Research Center to investigate methods for maintaining a laminar boundary layer on the wall of the nozzle to high unit Reybolds numbers. During these tests the disturbance levels in the inviscid flow and boundary-layer profiles were measured and were used to determine whether the boundary layer on the nozzle wall was laminar or turbulent. The disturbance levels were measured by using a constant-current hot-wire anemometer and a pitot probe. A pressure transducer, having a quartz sensing element and a low output impedance, was flush mounted at the end of the pitot probe to measure fluctuations in the pitot pressure. (See ref. 11 for a detailed description of transducers, probes, and data-reduction procedures.) The profiles of the mean pitot pressure in the boundary layer were measured by using a conventional pitot probe. The purpose of this appendix is to describe some of the transitional characteristics of the boundary layer on the wall of the Mach 5 nozzle.

The root-mean-square levels of the free-stream disturbances measured with the pitot probe and normalized by the mean free-stream pitot pressure are presented in figure 12. The measurements were made at three stations in the flow: 38.6, 50.0, and 62.7 cm downstream from the throat. (See fig. 13.) The length of the nozzle was 50.0 cm. The data in figure 12 show that the peak in the normalized disturbance levels measured at the three stations occurred at the same unit Reynolds number, $10/\mu m$. The unit Reynolds numbers were calculated by using conditions at the exit of the nozzle. Peak disturbance levels measured at the wall under a boundary layer that is undergoing transition occur near the end of transition (ref. 64); peak disturbances in the free stream due to noise radiated from a boundary layer undergoing transition would probably also occur near the end of transition. Therefore, the results presented in figure 12 indicate that those regions of the boundary layer that radiate noise to the probe located at the three stations became turbulent at the same pressure. Hence, transition was always initiated upstream of the pitot probe since disturbances produced by the boundary layer and measured by the probe are propagated along Mach waves. (See ref. 8.) For example, the disturbances from the boundary layer measured by the probe at the 38.6, 50.0, and 62.7 cm stations originated near the wall at and upstream of the 22.4, 32.9, and 43 cm stations,

respectively. (See fig. 13.) The pitot and hot-wire probes were located 1.27 cm from the center line of the tunnel; therefore, the locus determined by the acoustic origin from the wall to the probes defines a skewed plane across the nozzle as indicated by the dotted lines in figure 13.

To substantiate these results, a constant-current hot-wire anemometer with an uncalibrated wire was used to measure the relative free-stream disturbance levels. These results are shown in figure 14. The peaks of the disturbance levels measured at the three stations also occurred at about the same unit Reynolds number, and the value of the unit Reynolds number where the peaks occurred was about the same for the data measured by using the pitot probe $\left(R_\infty = 10/\mu m\right)$ and the hot-wire anemometer $\left(R_\infty = 10.8/\mu m\right)$. Therefore, the results from the hot-wire anemometer essentially confirm those obtained with the pitot probe.

Surveys were made with a conventional pitot probe to investigate further the behavior of the boundary layer on the wall of the nozzle. The profiles of the pitot pressure within the boundary layer measured at three stations are presented and compared with theory (ref. 40) in figure 15. The stations where the surveys were made are near the acoustic origin for the stations where the fluctuating pitot pressure and hot-wire anemometer measurements were made. (See fig. 13.)

When compared with the theoretical results, the trend of the pitot pressure profiles with increasing unit Reynolds number indicates that the boundary layers were essentially laminar at the first two stations for unit Reynolds numbers up to $10.08/\mu m$. At the 42.9-cm station, there is considerable disagreement between the laminar theory and the low Reynolds number data, and this disagreement might be caused by Taylor-Görtler vortices in the laminar boundary layer as discussed in the text of this report. However, the variation of the boundary-layer thickness with unit Reynolds number (that is, the decrease in boundary-layer thickness with increasing unit Reynolds number) suggests that the boundary layers were essentially laminar up to a unit Reynolds number of $10.08/\mu m$. A comparison of the measured profiles with theoretical values determined from turbulent theory indicates that transition definitely occurred at all stations for unit Reynolds numbers between $10.08/\mu m$ and $11.46/\mu m$. This result is consistent with the unit Reynolds numbers of $10/\mu m$ to $10.8/\mu m$ obtained for the peaks in the disturbance measurements made with the pitot probe and the hot-wire anemometer.

The measured pitot profiles indicated that the boundary layer was essentially laminar for unit Reynolds numbers up to $10.08/\mu m$. However, oscilloscope traces of the instantaneous output of the pressure transducer in the pitot probe (fig. 16) show sharp increases in the output of the transducer at random times during the tests for unit Reynolds numbers from $9.0/\mu m$ to $10.5/\mu m$ for the three measuring stations. (The total time indicated by the traces in figure 16 is only 10 msec; therefore, it is possible that sharp

increases occurred at lower unit Reynolds numbers and were not recorded. Because of this time limitation, the information obtained from these traces is very qualitative.) The character of the traces is similar to turbulent bursts measured at the wall under a transitional boundary layer. Therefore, the "turbulent bursts" shown by the traces are probably indicative of turbulent bursts in the boundary layer on the nozzle wall at the acoustic origin of the disturbances. Evidently, the disturbances in the transitional boundary layer are already large before the mean profiles change abruptly from laminar to turbulent shapes.

The three methods used to study the transitional characteristics of the boundary layer on the wall of the nozzle indicated that the boundary layer was either laminar, transitional, or turbulent for the length of the nozzle for which measurements were made. These results suggest that transition to turbulent flow always occurred upstream of the most forward acoustic origin, possibly in the neighborhood of the throat; and then turbulent flow persisted in the boundary layer downstream. (The possibility that transition in the nozzle was caused by Taylor-Görtler vortices as discussed in the text of this report is not yet resolved.) The initiation of turbulent flow at an upstream station and its subsequent propagation downstream is not a new observation. However, the apparent initiation of transitional processes in the boundary layer and their propagation downstream without becoming turbulent at some downstream station appear to be a new observation. This behavior might be explained by the action of a pressure gradient on the transitional boundary layer and by the increasing Mach number along the nozzle. Both of these effects would tend to damp disturbances and prevent the transitional boundary layer from becoming turbulent. These effects might be limited to small nozzles where the local Reynolds numbers do not become large enough to result in a turbulent boundary layer independent of its upstream history.

REFERENCES

1. Morkovin, Mark V.: Critical Evaluation of Transition from Laminar to Turbulent Shear Layers With Emphasis on Hypersonically Traveling Bodies. AFFDL-TR-68-149, U.S. Air Force, Mar. 1969. (Available from DDC as AD 686 178.)

2. Morkovin, Mark V.: On the Many Faces of Transition. Viscous Drag Reduction, C. Sinclair Wells, ed., Plenum Press, 1969, pp. 1-31.

3. Morkovin, M. V.: Critical Evaluation of Laminar-Turbulent Transition and High-Speed Dilemma. Vol. 13, Progress in Aerospace Sciences, D. Küchemann, ed., Pergamon Press, Inc., 1972.

4. Mack, Leslie M.: Boundary-Layer Stability Theory. 900-277 Rev. A (Contract No. NAS 7-100), Jet Propulsion Lab., California Inst. Technol., Nov. 1969.

5. Mack, Leslie M.; and Morkovin, Mark V.: High Speed Boundary-Layer Stability and Transition. AIAA Professional Study Series, 1969.

6. McCauley, W. D., ed.: Boundary Layer Transition Study Group Meeting. BSD-TR-67-213, Vols. I-IV, U.S. Air Force, Aug. 1967. (Available from DDC as AD 384 016, AD 820 364, AD 384 006, AD 384 017.)

7. Laufer, John: Aerodynamic Noise in Supersonic Wind Tunnels. J. Aerosp. Sci., vol. 28, no. 9, Sept. 1961, pp. 685-692.

8. Wagner, R. D., Jr.; Maddalon, D. V.; and Weinstein, L. M.: Influence of Measured Freestream Disturbances on Hypersonic Boundary-Layer Transition. AIAA J., vol. 8, no. 9, Sept. 1970, pp. 1664-1670.

9. Stainback, P. C.; Fischer, M. C.; and Wagner, R. D.: Effects of Wind-Tunnel Disturbances on Hypersonic Boundary-Layer Transition. Pts. I and II. AIAA Paper No. 72-181, Jan. 1972.

10. Beckwith, Ivan E.; and Bertram, Mitchel H.: A Survey of NASA Langley Studies on High-Speed Transition and the Quiet Tunnel. NASA TM X-2566, 1972.

11. Stainback, P. C.; and Wagner, R. D.: A Comparison of Disturbance Levels Measured in Hypersonic Tunnels Using a Hot-Wire Anemometer and a Pitot Pressure Probe. AIAA Paper No. 72-1003, Sept. 1972.

12. Fischer, M. C.; and Wagner, R. D.: Transition and Hot-Wire Measurements in Hypersonic Helium Flow. AIAA J., vol. 10, no. 10, Oct. 1972, pp. 1326-1332.

13. Bergstrom, E. R.; and Raghunathan, S.: Aerodynamic Noise and Boundary-Layer Transition Measurements in Supersonic Test Facilities. AIAA J., vol. 10, no. 10, Oct. 1972, pp. 1531-1532.

14. Stainback, P. Calvin; Wagner, Richard D.; Owen, F. Kevin; and Horstman, Clifford C.: Experimental Studies of Hypersonic Boundary-Layer Transition and Effects of Wind-Tunnel Disturbances. NASA TN D-7453, 1974.

15. Boldman, Donald R.; Schmidt, James F.; and Gallagher, Anne K.: Laminarization of a Turbulent Boundary Layer as Observed From Heat-Transfer and Boundary-Layer Measurements in Conical Nozzles. NASA TN D-4788, 1968.

16. Back, L. H.; Cuffel, R. F.; and Massier, P. F.: Laminarization of a Turbulent Boundary Layer in Nozzle Flow – Boundary Layer and Heat Transfer Measurements With Wall Cooling. Trans. ASME, Ser. C: J. Heat Transfer, vol. 92, no. 3, Aug. 1970, pp. 333-344.

17. Nash-Webber, J. L.; and Oates, G. C.: An Engineering Approach to the Design of Laminarizing Nozzle Flows. Trans. ASME, Ser. D: J. Basic Eng., vol. 94, no. 4, Dec. 1972, pp. 897-903.

18. Witte, Arvel B.; and Harper, Edward Y.: Experimental Investigation of Heat Transfer Rates in Rocket Thrust Chambers. AIAA J., vol. 1, no. 2, Feb. 1963, pp. 443-451.

19. Back, Lloyd H.; Cuffel, Robert F.; and Massier, Paul F.: Influence of Contraction Section Shape and Inlet Flow Direction on Supersonic Nozzle Flow and Performance. J. Spacecraft & Rockets, vol. 9, no. 6, June 1972, pp. 420-427.

20. Turner, A. B.: Local Heat Transfer Measurements on a Gas Turbine Blade. J. Mech. Eng., vol. 13, no. 1, Feb. 1971, pp. 1-12.

21. McDonald, H.; and Fish, R. W.: Practical Calculations of Transitional Boundary Layers. Rep. L110887-1, Res. Lab., United Aircraft Corp., Mar. 1972.

22. Kestin, J.; and Richardson, P. D.: The Effects of Free-Stream Turbulence and of Sound Upon Heat Transfer. ARL-69-0062, U.S. Air Force, Apr. 1969. (Available from DDC as AD 691 497.)

23. Kestin, J.; and Wood, R. T.: Enhancement of Stagnation-Line Heat Transfer by Turbulence. Vol. 2, Progress in Heat and Mass Transfer, Thomas F. Irvine, Jr., Warren E. Ibele, James P. Hartnett, and Richard J. Goldstein, eds., Pergamon Press, Inc., c.1969, pp. 249-253.

24. Gostkowski, Vincent J.; and Costello, Frederick A.: The Effect of Free Stream Turbulence on the Heat Transfer From the Stagnation Point of a Sphere. Int. J. Heat & Mass Transfer, vol. 13, no. 8, Aug. 1970, pp. 1382-1386.

25. Dods, Jules B., Jr.; and Hanly, Richard D.: Evaluation of Transonic and Supersonic Wind-Tunnel Background Noise and Effects of Surface Pressure Fluctuation Measurements. AIAA Paper No. 72-1004, Sept. 1972.

26. Sternberg, Joseph: The Transition From a Turbulent to a Laminar Boundary Layer. Rep. No. 906, Ballistic Res. Lab., Aberdeen Proving Ground, May 1954.

27. Launder, Brian E.: Laminarization of the Turbulent Boundary Layer by Acceleration. Rep. No. 77, Gas Turbine Lab., Massachusetts Inst. Technol., Nov. 1964.

28. Moretti, P. M.; and Kays, W. M.: Heat Transfer to a Turbulent Boundary Layer With Varying Free-Stream Velocity and Varying Surface Temperature – An Experimental Study. Int. J. Heat & Mass Transfer, vol. 8, no. 9, Sept. 1965, pp. 1187-1202.

29. Kline, S. J.; Reynolds, W. C.; Schraub, F. A.; and Runstadler, P. W.: The Structure of Turbulent Boundary Layers. J. Fluid Mech., vol. 30, pt. 4, Dec. 22, 1967, pp. 741-773.

30. Badri Narayanan, M. A.; and Ramjee, V.: On the Criteria for Reverse Transition in a Two-Dimensional Boundary Layer Flow. J. Fluid Mech., vol. 35, pt. 2, Feb. 3, 1969, pp. 225-241.

31. Launder, B. E.; and Jones, W. P.: On the Prediction of Laminarisation. C.P. No. 1036, Brit. A.R.C., 1969.

32. Jones, W. P.; and Launder, B. E.: The Prediction of Laminarization With a Two-Equation Model of Turbulence. Int. J. Heat & Mass Transfer, vol. 15, no. 2, Feb. 1972, pp. 301-314.

33. Lighthill, M. J.: Sound Generated Aerodynamically. Proc. Roy. Soc. London, Ser. A, vol. 267, no. 1329, May 8, 1962, pp. 147-182.

34. Ffowcs Williams, J. E.: The Noise From Turbulence Convected at High Speed. Phil. Trans. Roy. Soc. London, Ser. A, vol. 255, no. 1061, Apr. 18, 1963, pp. 469-503.

35. Jones, W. P.; and Launder, B. E.: Some Properties of Sink-Flow Turbulent Boundary Layers. J. Fluid Mech., vol. 56, pt. 2, 1972, pp. 337-351.

36. Blackwelder, Ron F.; and Kovasznay, Leslie S. G.: Large-Scale Motion of a Turbulent Boundary Layer During Relaminarization. J. Fluid Mech., vol. 53, pt. 1, May 9, 1972, pp. 61-83.

37. Amick, James L.; and Karvelis, Albertas V.: Preliminary Tests of a 6.6-Inch Diameter Mach 8 Wind Tunnel. WTM 288, ORA Project 07222 (Contract No. No. AF 33(615)2407), Univ. of Michigan, May 1967.

38. Winkler, E. M.; and Persh, Jerome: Experimental and Theoretical Investigation of the Boundary Layer and Heat Transfer Characteristics of a Cooled Hypersonic Wedge Nozzle at a Mach Number of 5.5. NAVORD Rep. 3757, U.S. Navy, July 8, 1954.

39. Nash-Webber, James Ludlow: Wall Shear-Stress and Laminarisation in Accelerated Turbulent Compressible Boundary-Layers. Rep. No. 94, Gas Turbine Lab., Massachusetts Inst. Technol., Apr. 1968.

40. Harris, Julius E.: Numerical Solution of the Equations for Compressible Laminar, Transitional, and Turbulent Boundary Layers and Comparisons With Experimental Data. NASA TR R-368, 1971.

41. Hall, D. J.; and Gibbings, J. C.: Influence of Stream Turbulence and Pressure Gradient Upon Boundary Layer Transition. J. Mech. Eng. Sci., vol. 14, no. 2, Apr. 1972, pp. 134-146.

42. Kays, W. M.; Moffat, R. J.; and Thielbahr, W. H.: Heat Transfer to the Highly Accelerated Turbulent Boundary Layer With and Without Mass Addition. 69-HT-53, ASME, Aug. 1969.

43. Wilson, D. G.; and Pope, J. A.: Convective Heat Transfer to Gas Turbine Blade Surfaces. Proc. Inst. Mech. Eng. (London), vol. 168, no. 36, 1954, pp. 861-876.

44. Wesoky, Howard L.; and May, Charlene: Boundary Layer Measurements in an Accelerated Flow With and Without Heat Transfer. NASA TN D-7030, 1971.

45. Back, L. H.; Cuffel, R. F.; and Massier, P. F.: Laminarization of a Turbulent Boundary Layer in Nozzle Flow. AIAA J., vol. 7, no. 4, Apr. 1969, pp. 730-733.

46. Brinich, Paul F.; and Neumann, Harvey E.: Some Characteristics of Turbulent Boundary Layers in Rapidly Accelerated Flows. NASA TN D-6587, 1971.

47. Hopkins, D. F.; and Hill, D. E.: Effect of Small Radius of Curvature on Transonic Flow in Axisymmetric Nozzles. AIAA J., vol. 4, no. 8, Aug. 1966, pp. 1337-1343.

48. Beckwith, Ivan E.; Ridyard, Herbert W.; and Cromer, Nancy: The Aerodynamic Design of High Mach Number Nozzles Utilizing Axisymmetric Flow With Application to a Nozzle of Square Test Section. NACA TN 2711, 1952.

49. Prozan, R. J.: Solution of Non-Isoenergetic Supersonic Flows by Method of Characteristics. LMSC-HREC D162220-III-A (Contract NAS 7-761), Lockheed Missiles & Space Co., July 1971. (Available as NASA CR-132274.)

50. Morkovin, M. V.: On Supersonic Wind Tunnels With Low Free-Stream Disturbances. Trans. ASME, Ser. E.: J. Appl. Mech., vol. 26, no. 3, Sept. 1959, pp. 319-323.

51. Groth, E. E.: Boundary Layer Suction Experiments at Supersonic Speeds. Boundary Layer and Flow Control. Vol. 2, G. V. Lachmann, ed., Pergamon Press, Inc., 1961, pp. 1049-1076.

52. Hixon, Barbara A.; Beckwith, Ivan E.; and Bushnell, Dennis M.: Computer Program For Compressible Laminar or Turbulent Nonsimilar Boundary Layers. NASA TM X-2140, 1971.

53. Shamroth, S. J.; and McDonald H.: Assessment of a Transitional Boundary Layer Theory at Low Hypersonic Mach Numbers. NASA CR-2131, 1972.

54. Uberoi, Mahinder S.: Effect of Wind-Tunnel Contraction on Free-Stream Turbulence. J. Aeronaut. Sci., vol. 23, no. 8, Aug. 1956, pp. 754-764.

55. Spangler, J. G.; and Wells, C. S., Jr.: Effects of Freestream Disturbances on Boundary-Layer Transition. AIAA J., vol. 6, no. 3, Mar. 1968, pp. 543-545.

56. Lukasiewicz, J.: Elimination of Flow Instability in Two High-Speed Wind Tunnels by Means of High-Drag Screens. LR-83, Nat. Aeronaut. Estab. Canada, Nov. 1953.

57. Jones, Robert A.; and Feller, William V.: Preliminary Surveys of the Wall Boundary Layer in a Mach 6 Axisymmetric Tunnel. NASA TN D-5620, 1970.

58. Loehrke, R. I.; and Nagib, H. M.: Experiments on Management of Free Stream Turbulence. AGARD Rep. 598, Sept. 1972.

59. Bradshaw, P.: The Effect of Wind-Tunnel Screens on Nominally Two-Dimensional Boundary Layers. J. Fluid Mech., vol. 22, pt. 4, Aug. 1965, pp. 679-687.

60. Rotta, J. C.: Effect of Streamwise Wall Curvature on Compressible Turbulent Boundary Layers. Phys. Fluids Suppl., vol. 10, pt. II, no. 9, Sept. 1967, pp. S174-S180.

61. Kobayashi, Ryóji: Note on the Stability of a Boundary Layer on a Concave Wall With Suction. J. Fluid Mech., vol. 52, pt. 2, Mar. 28, 1972, pp. 269-272.

62. Smith, A. M. O.: On the Growth of Taylor-Görtler Vortices Along Highly Concave Walls. Quart. Appl. Math., vol. XIII, no. 3, Oct. 1955, pp. 233-262.

63. Schlichting, Hermann (J. Kestin, transl.): Boundary-Layer Theory. Sixth ed., McGraw-Hill Book Co., Inc., 1968, pp. 505-507.

64. Owen, F. K.: Transition Experiments on a Flat Plate at Subsonic and Supersonic Speeds. AIAA J., vol. 8, no. 3, Mar. 1970, pp. 518-523.

TABLE I.- NOZZLE COORDINATES AND FLOW VARIABLES

[Values for y_* given in table II]

(a) JPL 20-inch tunnel (ref. 7)

x/y_*	s/y_*	y/y_*	M_e from one-dimensional solution	x/y_*	s/y_*	y/y_*	M_e from one-dimensional solution
-50.2703	-43.3112	14.9557	0.039	25.2259	35.3137	2.9600	2.623
-41.4400	-32.7997	9.5005	.061	27.0270	37.1318	3.2130	2.710
-39.6389	-30.7553	8.6984	.067	28.8303	38.9533	3.4746	2.792
-37.8378	-28.7927	7.9416	.071	30.6314	40.7740	3.7470	2.872
-36.0346	-26.8455	7.2303	.080	32.4324	42.5961	4.0260	2.953
-34.2335	-24.9173	6.5643	.089	34.2357	44.4213	4.3114	3.019
-32.4324	-23.0043	5.9416	.098	36.0368	46.2454	4.6032	3.088
-30.6292	-21.1030	5.3600	.109	37.8378	48.0705	4.9016	3.154
-28.8281	-19.2165	4.8195	.121	39.6411	49.8984	5.2022	3.216
-27.0270	-17.3418	4.3200	.135	41.4422	51.7246	5.5049	3.276
-25.2238	-15.4756	3.8595	.152	43.2432	53.5513	5.8119	3.334
-23.4227	-13.6212	3.4378	.171	45.0465	55.3794	6.1060	3.387
-21.6216	-11.7755	3.0530	.194	46.3178	56.6694	6.3351	3.426
-19.8184	-9.9354	2.7070	.220	47.7254	58.0985	6.5751	3.466
-18.0173	-8.1044	2.3935	.251	50.7524	61.1687	7.0854	3.546
-16.2162	-6.2791	2.1155	.287	52.3805	62.8196	7.3578	3.587
-14.4130	-4.4569	1.8709	.330	54.0886	64.5513	7.6411	3.627
-12.6119	-2.6414	1.6588	.380	55.8832	66.3703	7.9373	3.669
-10.8108	-.8296	1.4781	.438	57.7665	68.2785	8.2422	3.710
-9.0076	.9813	1.3278	.506	59.7405	70.2779	8.5578	3.751
-7.2065	2.7876	1.2071	.585	61.8097	72.3729	8.8822	3.791
-5.4054	4.5918	1.1150	.673	63.9827	74.5720	9.2173	3.832
-3.6022	6.3968	1.0506	.773	66.2573	76.8731	9.5632	3.873
-1.8011	8.1987	1.0125	.882	68.6422	79.2846	9.9157	3.913
.0000	10.0000	1.0000	1.000	71.1395	81.8083	10.2746	3.953
1.8032	11.8033	1.0121	1.124	73.7557	84.4508	10.6422	3.992
3.6043	13.6046	1.0478	1.253	76.4930	87.2142	11.0141	4.030
5.4054	15.4063	1.1062	1.384	79.3578	90.1045	11.3903	4.068
7.2086	17.2109	1.1862	1.515	82.3524	93.1238	11.7686	4.105
9.0097	19.0143	1.2867	1.644	85.4811	96.2764	12.1492	4.141
10.8108	20.8188	1.4071	1.770	88.7503	99.5686	12.5276	4.176
12.6141	22.6267	1.5460	1.893	89.1373	99.9582	12.5730	4.180
14.4151	24.4338	1.7027	2.011	92.1643	103.0048	12.9059	4.210
16.2162	26.2425	1.8761	2.124	95.7297	106.5907	13.2800	4.243
18.0195	28.0548	2.0651	2.233	99.4508	110.3311	13.6476	4.274
19.8205	29.8666	2.2681	2.337	103.3362	114.2344	14.0108	4.305
21.6216	31.6799	2.4865	2.437	107.3946	118.3093	14.3654	4.333
23.4249	33.4972	2.7178	2.532	111.6324	127.0040	14.6249	4.354

TABLE I.- NOZZLE COORDINATES AND FLOW VARIABLES – Continued

(b) 22-inch helium tunnel (ref. 8)

x/y_*	s/y_*	y/y_*	M_e from one-dimensional flow	x/y_*	s/y_*	y/y_*	M_e from one-dimensional flow
-3.9517	5.3754	2.6702	0.079	149.1553	159.7139	10.5170	11.937
-2.8169	6.9019	1.7786	.182	155.3414	165.9006	10.6066	12.007
-2.1895	7.6623	1.4184	.296	161.5289	172.0887	10.6777	12.061
-.7655	9.2205	1.0364	.721	168.4902	179.0505	10.7669	12.131
.0000	10.0000	1.0000	1.000	174.6790	185.2398	10.8462	12.191
.7745	10.7751	1.0165	1.225	181.6419	192.2032	10.9336	12.259
1.5484	11.5502	1.0790	1.528	187.8318	198.3935	10.9952	12.306
3.0852	13.0976	1.3026	2.157	194.7970	205.3591	11.0617	12.357
3.8481	13.8708	1.4418	2.458	200.9885	211.5509	11.1410	12.417
4.6090	14.6450	1.5878	2.742	207.1800	217.7428	11.1947	12.459
5.3689	15.4194	1.7407	3.016	214.1459	224.7092	11.2843	12.526
6.8865	16.9673	2.0439	3.510	220.3386	230.9025	11.3819	12.601
8.4027	18.5134	2.3469	3.961	226.5308	237.0953	11.4408	12.645
9.9179	20.0584	2.6481	4.378	233.4987	244.0636	11.5226	12.707
11.4324	21.6025	2.9489	4.773	239.6925	250.2582	11.6456	12.799
12.9465	23.1453	3.2407	5.137	245.8864	256.4527	11.6796	12.825
15.9780	26.2296	3.7921	5.789	252.8558	263.4224	11.7565	12.882
19.7739	30.0825	4.4200	6.484	259.0512	269.6183	11.8543	12.956
22.8183	33.1643	4.8729	6.961	265.2465	275.8143	11.9343	13.015
26.6317	37.0164	5.3940	7.489	272.2171	282.7854	12.0124	13.074
29.6873	40.0977	5.7704	7.858	278.0259	288.5948	12.1154	13.150
32.7460	43.1781	6.1226	8.195	291.5808	302.1514	12.2928	13.281
35.8086	46.2600	6.4589	8.511	297.7773	308.3490	12.4321	13.383
38.8739	49.3419	6.7607	8.788	303.9739	314.5470	12.5615	13.479
42.7090	53.1905	7.0136	9.018	310.9449	321.5190	12.6530	13.545
45.7797	56.2675	7.2058	9.189	317.1422	327.7172	12.7762	13.635
48.8520	59.3465	7.4187	9.378	323.3395	333.9156	12.8836	13.713
51.9259	62.4274	7.6222	9.557	330.3120	340.8889	12.9651	13.772
55.0016	65.5095	7.8131	9.723	336.5105	347.0881	13.0807	13.855
58.8476	69.3625	8.0392	9.917	342.7086	353.2873	13.1998	13.942
61.9257	72.4453	8.2001	10.055	349.6819	360.2620	13.3413	14.043
65.0061	75.5297	8.3525	10.184	355.8819	366.4638	13.5115	14.165
68.0865	78.6139	8.5040	10.312	362.0781	372.6614	13.5865	14.218
71.1681	81.6988	8.6374	10.423	369.0533	379.6380	13.7636	14.344
74.2509	84.7845	8.7742	10.537	375.2545	385.8421	13.9795	14.496
78.1046	88.6417	8.9308	10.666	381.4480	392.0381	14.1147	14.592
82.7301	93.2707	9.1025	10.808	388.4248	399.0164	14.2447	14.682
87.2636	97.8077	9.2824	10.954	394.6260	405.2186	14.3509	14.757
92.7578	103.3049	9.4200	11.067	400.8233	411.4206	14.6772	14.984
97.3880	107.9366	9.5442	11.166	414.0013	424.6095	14.8515	15.104
102.0201	112.5702	9.6637	11.263	420.1986	430.8119	14.9820	15.195
107.4247	117.9765	9.7872	11.361	427.1754	437.7921	15.2516	15.379
112.0591	122.6119	9.8776	11.434	433.3766	443.9973	15.4592	15.521
116.6935	127.2472	9.9634	11.502	439.5739	450.1969	15.5765	15.601
121.3298	131.8844	10.0600	11.579	446.5507	457.1754	15.7412	15.713
126.7394	137.2952	10.1724	11.667	452.7519	463.3794	15.9663	15.864
129.8304	140.3866	10.2172	11.703	458.9492	469.5797	16.1149	15.965
136.0133	146.5703	10.3202	11.783	465.9260	476.5599	16.3766	16.139
142.1971	152.7549	10.4196	11.861	469.8003	480.4409	16.6625	16.330

TABLE I.- NOZZLE COORDINATES AND FLOW VARIABLES – Continued

(c) 6.6-inch Mach 8 tunnel (ref. 37)

x/y_*	s/y_*	y/y_*	M_e from series solution and method of characteristics	x/y_*	s/y_*	y/y_*	M_e from series solution and method of characteristics
-5.2663	0.8932	6.5963	0.009	0.8019	10.8031	1.0407	1.404
-5.2475	1.0378	6.4548	.010	.9349	10.9368	1.0564	1.476
-5.2283	1.1825	6.3133	.010	1.0674	11.0704	1.0745	1.550
-5.2085	1.3276	6.1719	.011	1.1995	11.2039	1.0953	1.627
-5.1880	1.4727	6.0305	.011	1.3310	11.3372	1.1187	1.707
-5.1667	1.6182	5.8894	.012	1.4325	11.4405	1.1387	1.772
-5.1446	1.7637	5.7483	.012	1.5270	11.5370	1.1590	1.835
-5.0269	2.4805	5.0860	.016	1.6332	11.6459	1.1838	1.911
-4.8831	3.2250	4.4347	.023	1.7536	11.7699	1.2149	2.005
-4.7453	3.7930	3.9570	.030	1.8913	11.9127	1.2549	2.130
-4.6144	4.2227	3.5928	.038	2.0526	12.0820	1.3104	2.316
-4.4874	4.5672	3.3064	.046	2.2438	12.2860	1.3872	2.476
-4.3636	4.8509	3.0752	.054	2.4659	12.5265	1.4823	2.601
-4.2441	5.0901	2.8845	.062	2.7225	12.8062	1.5945	2.721
-4.1291	5.2968	2.7246	.070	3.0191	13.1302	1.7256	2.842
-4.0192	5.4784	2.5887	.079	3.3629	13.5059	1.8774	2.967
-3.9146	5.6399	2.4719	.088	3.7622	13.9423	2.0523	3.098
-3.8153	5.7852	2.3708	.097	4.2285	14.4507	2.2534	3.235
-3.7214	5.9167	2.2824	.106	4.7749	15.0446	2.4838	3.380
-3.6325	6.0366	2.2051	.115	5.4174	15.7405	2.7469	3.534
-3.5487	6.1463	2.1364	.125	6.1765	16.5586	3.0466	3.696
-3.4693	6.2477	2.0754	.136	7.0760	17.5230	3.3869	3.868
-2.9719	6.8593	1.7479	.197	8.1454	18.6629	3.7716	4.049
-2.4196	7.4987	1.4718	.289	9.4197	20.0129	4.2043	4.242
-1.8247	8.1473	1.2582	.413	10.9410	21.6145	4.6882	4.445
-1.6999	8.2783	1.2232	.443	12.7554	23.5125	5.2249	4.658
-1.5740	8.4087	1.1908	.476	14.9195	25.7624	5.8149	4.881
-1.4468	8.5397	1.1609	.510	17.4942	28.4235	6.4565	5.113
-1.3187	8.6710	1.1335	.547	20.5453	31.5597	7.1456	5.352
-1.1897	8.8027	1.1087	.585	24.1374	35.2335	7.8742	5.597
-1.0597	8.9347	1.0864	.625	28.3340	39.5068	8.6314	5.845
-.9290	9.0671	1.0667	.668	33.1890	44.4314	9.4029	6.093
-.7977	9.1998	1.0496	.712	38.7399	50.0437	10.1720	6.336
-.6658	9.3327	1.0350	.759	44.9836	56.3394	10.9185	6.572
-.5333	9.4658	1.0230	.808	51.9449	63.3433	11.6286	6.798
-.4004	9.5992	1.0134	.858	59.5158	70.9478	12.2801	7.008
-.2672	9.7326	1.0064	.911	67.6053	79.0629	12.8608	7.200
-.1337	9.8663	1.0020	.965	76.0629	87.5388	13.3617	7.371
.0000	10.0000	1.0000	1.022	84.6836	96.1720	13.7788	7.520
.1338	10.1338	1.0005	1.080	93.2944	104.7911	14.1167	7.645
.2676	10.2677	1.0035	1.141	101.6302	113.1321	14.3811	7.748
.4015	10.4016	1.0091	1.203	109.4464	120.9516	14.5825	7.829
.5351	10.5354	1.0171	1.268	109.9054	121.4111	14.5931	7.833
.6687	10.6693	1.0277	1.335	110.3650	121.8707	14.6035	7.837

TABLE I.- NOZZLE COORDINATES AND FLOW VARIABLES – Continued

(d) 4-inch Mach 5 nozzle (Langley Research Center); measured coordinates

x/y_*	s/y_*	y/y_*	M_e from one-dimensional solution	x/y_*	s/y_*	y/y_*	M_e from one-dimensional solution
-9.8363	0.1637	4.5680	0.028	21.2797	31.2796	3.9983	4.458
-8.4784	1.5215	3.6736	.043	21.9100	31.9100	4.0639	4.496
-7.2505	2.7495	2.9522	.067	22.5424	32.5424	4.1266	4.533
-6.2629	3.7371	2.4264	.099	23.1746	33.1746	4.1885	4.568
-5.2864	4.7135	2.0213	.143	23.8065	33.8065	4.2454	4.600
-4.3502	5.6498	1.6913	.208	24.4382	34.4382	4.3022	4.632
-3.4494	6.5506	1.4338	.297	25.0723	35.0723	4.3570	4.663
-2.5789	7.4211	1.2462	.412	25.7038	35.7038	4.4126	4.693
-1.7079	8.2921	1.0965	.588	26.3354	36.3354	4.4685	4.723
-.8508	9.1492	1.0195	.797	26.9691	36.9691	4.5155	4.749
.0000	10.0000	1.0000	1.000	27.6000	37.6000	4.5639	4.775
.0253	10.0253	1.0001	1.008	28.2309	38.2309	4.6084	4.798
.1036	10.1036	1.0002	1.012	28.8640	38.8640	4.6514	4.821
.2627	10.2627	1.0003	1.026	29.4970	39.4970	4.6918	4.842
.4194	10.4194	1.0023	1.075	30.1274	40.1274	4.7307	4.863
.5786	10.5786	1.0056	1.119	30.7600	40.7600	4.7620	4.879
.7353	10.7353	1.0106	1.166	31.3925	41.3925	4.7969	4.897
1.0513	11.0513	1.0213	1.240	32.0226	42.0226	4.8307	4.914
1.6837	11.6837	1.0601	1.416	32.6550	42.6549	4.8586	4.928
2.3144	12.3145	1.1114	1.581	33.2874	43.2874	4.8914	4.945
2.9438	12.9438	1.1780	1.751	33.9198	43.9198	4.9217	4.961
3.5771	13.5771	1.2557	1.917	34.5495	44.5495	4.9470	4.973
4.2068	14.2068	1.3456	2.083	35.1817	45.1817	4.9747	4.987
4.8404	14.8404	1.4432	2.243	35.8139	45.8139	5.0000	5.000
5.4723	15.4723	1.5449	2.392	36.4460	46.4459	5.0203	5.010
6.1025	16.1025	1.6516	2.536	37.0779	47.0780	5.0430	5.021
6.7358	16.7358	1.7607	2.672	37.7100	47.7100	5.0657	5.032
7.3670	17.3671	1.8722	2.801	38.1675	48.1675	5.0758	5.038
7.9985	17.9985	1.9834	2.922	38.3419	48.3419	5.0809	5.040
8.6324	18.6324	2.0945	3.037	38.9738	48.9738	5.1011	5.050
9.2638	19.2638	2.2059	3.146	39.6058	49.6058	5.1168	5.058
9.8953	19.8953	2.3181	3.251	40.2376	50.2376	5.1355	5.067
10.5271	20.5271	2.4323	3.353	40.8695	50.8695	5.1496	5.074
11.1616	21.1616	2.5480	3.452	41.5013	51.5013	5.1663	5.082
11.7934	21.7934	2.6592	3.544	42.1331	52.1331	5.1779	5.088
12.4247	22.4246	2.7688	3.631	42.7649	52.7649	5.1941	5.096
13.0580	23.0581	2.8752	3.713	43.3967	53.3967	5.2024	5.100
13.6909	23.6909	2.9795	3.791	44.0284	54.0284	5.2160	5.106
14.3235	24.3235	3.0816	3.865	44.6576	54.6576	5.2214	5.108
14.9557	24.9557	3.1819	3.936	45.2893	55.2893	5.2317	5.114
15.5874	25.5874	3.2769	4.002	45.9211	55.9211	5.2373	5.116
16.2211	26.2211	3.3724	4.067	46.5527	56.5527	5.2472	5.121
16.8546	26.8546	3.4626	4.126	47.1844	57.1843	5.2537	5.124
17.4875	27.4875	3.5510	4.184	47.8161	57.8160	5.2613	5.128
18.1197	28.1197	3.6301	4.234	48.4478	58.4478	5.2767	5.136
18.7511	28.7511	3.7077	4.283	49.0795	59.0796	5.2843	5.139
19.3824	29.3824	3.7828	4.329	49.7113	59.7113	5.2982	5.146
20.0133	30.0133	3.8555	4.373	50.0096	60.0009	5.3116	5.152
20.6465	30.6465	3.9265	4.416				

TABLE I.- NOZZLE COORDINATES AND FLOW VARIABLES – Continued

(e) Rapid-expansion Mach 5 nozzle; design coordinates

x/y_*	s/y_*	y/y_*	M_e from series solution and method of characteristics	x/y_*	s/y_*	y/y_*	M_e from series solution and method of characteristics
-5.1518	1.7974	6.8999	0.014	-0.4686	9.2809	1.4731	0.286
-4.7107	2.2404	6.8495	.014	-.4383	9.3518	1.3975	.333
-4.4967	2.4577	6.8017	.014	-.4105	9.4231	1.3359	.380
-4.3204	2.6397	6.7512	.014	-.3854	9.4821	1.2848	.427
-4.1666	2.8006	6.7010	.015	-.3603	9.5354	1.2418	.473
-3.9299	3.0538	6.6001	.015	-.3377	9.5792	1.2056	.520
-3.5496	3.4751	6.4012	.016	-.3150	9.6199	1.1744	.567
-3.2497	3.8250	6.1995	.017	-.2923	9.6567	1.1475	.614
-3.0003	4.1347	6.0006	.018	-.2718	9.6882	1.1242	.662
-2.7963	4.4077	5.8017	.018	-.2509	9.7184	1.1043	.710
-2.6049	4.6803	5.6001	.019	-.2304	9.7462	1.0865	.758
-2.4359	4.9336	5.4012	.020	-.2101	9.7723	1.0713	.808
-2.2848	5.1763	5.1995	.022	-.1901	9.7967	1.0580	.858
-2.1463	5.4129	5.0006	.024	-.1705	9.8199	1.0466	.910
-2.0154	5.6466	4.8014	.026	-.1511	9.8420	1.0363	.963
-1.9057	5.8611	4.6004	.028	-.1321	9.8632	1.0278	1.017
-1.7594	6.1578	4.3522	.031	-.1137	9.8832	1.0206	1.073
-1.6188	6.4458	4.0880	.035	-.0952	9.9029	1.0145	1.131
-1.4779	6.7523	3.8083	.040	-.0774	9.9215	1.0097	1.192
-1.3374	7.0711	3.5151	.047	-.0596	9.9398	1.0061	1.254
-1.1965	7.4029	3.2083	.057	-.0453	9.9543	1.0030	1.320
-1.0559	7.7456	2.8894	.070	-.0251	9.9749	1.0012	1.388
-.9855	7.9224	2.7249	.078	-.0085	9.9915	1.0003	1.460
-.9151	8.1022	2.5583	.089	.0000	10.0000	1.0000	1.500
-.8449	8.2842	2.3885	.102	.0151	10.0151	1.0007	1.528
-.7745	8.4693	2.2168	.119	.0459	10.0460	1.0015	1.536
-.7276	8.5933	2.1013	.125	.1049	10.1050	1.0051	1.543
-.6808	8.7184	1.9849	.149	.1699	10.1702	1.0110	1.551
-.6339	8.8441	1.8679	.169	.2403	10.2410	1.0197	1.564
-.5871	8.9703	1.7506	.193	.2966	10.2978	1.0280	1.575
-.5399	9.0972	1.6330	.224	.3440	10.3458	1.0358	1.589
-.4930	9.2234	1.5154	.263	.3984	10.4010	1.0456	1.610

TABLE I.- NOZZLE COORDINATES AND FLOW VARIABLES – Concluded

(e) Rapid-expansion Mach 5 nozzle; design coordinates – Concluded

x/y_*	s/y_*	y/y_*	M_e from series solution and method of characteristics	x/y_*	s/y_*	y/y_*	M_e from series solution and method of characteristics
0.4562	10.4598	1.0568	1.632	7.8422	18.1405	2.9953	3.623
.5085	10.5131	1.0676	1.655	8.6859	19.0004	3.1566	3.721
.5680	10.5740	1.0806	1.687	9.2956	19.6207	3.2672	3.787
.6312	10.6387	1.0949	1.721	9.8222	20.1552	3.3555	3.840
.6880	10.6970	1.1081	1.753	10.4646	20.8064	3.4613	3.901
.7530	10.7638	1.1236	1.788	11.1345	21.4848	3.5647	3.961
.8198	10.8326	1.1404	1.823	11.7116	22.0684	3.6502	4.010
.8800	10.8946	1.1557	1.855	12.4093	22.7734	3.7485	4.066
.9492	10.9661	1.1733	1.892	13.1372	23.5081	3.8443	4.122
1.0203	11.0394	1.1919	1.928	13.7597	24.1356	3.9223	4.166
1.0840	11.1054	1.2087	1.960	14.5103	24.8917	4.0106	4.218
1.1551	11.1790	1.2282	1.993	15.2911	25.6777	4.0986	4.268
1.2322	11.2587	1.2483	2.032	15.9537	26.3442	4.1666	4.309
1.3068	11.3489	1.3195	2.067	16.7548	27.1493	4.2449	4.355
1.5166	11.6031	1.3805	2.162	17.5810	27.9792	4.3204	4.401
1.7080	11.8024	1.4359	2.246	18.2790	28.6799	4.3809	4.438
1.8945	11.9964	1.4888	2.327	19.1203	29.5242	4.4489	4.480
2.0807	12.1903	1.5442	2.403	19.9994	30.4058	4.5118	4.522
2.2672	12.3849	1.5997	2.485	20.5840	30.9919	4.5520	4.548
2.4563	12.5819	1.6551	2.548	21.5940	32.0041	4.6176	4.591
2.6527	12.7867	1.7130	2.622	22.5060	32.9179	4.6705	4.628
2.7987	12.9389	1.7558	2.674	23.1106	33.5234	4.7031	4.651
2.8340	12.9757	1.7659	2.687	24.1536	34.5678	4.7561	4.689
3.0330	13.1828	1.8239	2.751	25.0931	35.5084	4.7966	4.722
3.2421	13.4009	1.8869	2.813	25.7128	36.1286	4.8216	4.742
3.4438	13.6108	1.9423	2.866	26.7382	37.1548	4.8594	4.773
3.9247	14.1101	2.0783	2.983	28.0556	38.4730	4.8996	4.811
4.4565	14.6618	2.2219	3.097	29.3706	39.7885	4.9350	4.845
5.0357	15.2607	2.3705	3.209	30.7488	41.1671	4.9652	4.878
5.6657	15.9102	2.5242	3.317	31.4063	41.8247	4.9779	4.892
6.3431	16.6064	2.6804	3.423	32.0586	42.4771	4.9879	4.906
7.0713	17.3528	2.8391	3.525				

TABLE II.- VALUES OF R_{ref}, R_{∞}, AND STAGNATION CONDITIONS FOR LAMINAR OR TRANSITIONAL FLOW IN SEVERAL NOZZLES

Nozzle	Reference	M_{∞}	y_*		p_o		T_o		R_{ref}	R_{∞}		Comments
			cm	in.	N/cm^2	psia	K	^oR		per m	per ft	
JPL 20-inch tunnel	*7	2.4	10.03	3.95	0.7	1.0	294	530	1.4×10^5	0.7×10^6	0.2×10^6	Laminar to nozzle exit,
		3.7	2.95	1.16	1.9	2.7	↓	↓	1.1	1.0	.3	$x \approx 355$ cm (140 in.)
		4.6	1.45	.57	5.3	7.7	↓	↓	1.6	1.9	.6	
University of Michigan (contoured nozzle)	†37	8.0	.56	.22	68.9	90.0	700	1260	2.5	1.5	.5	Laminar to nozzle exit, $x \approx 86$ cm (34 in.)
University of Michigan (conical nozzle)	†37	9.2	.43	.17	107	156	860	1550	3.3	1.3	.4	Laminar to nozzle exit, $x \approx 76$ cm (30 in.)
Langley 22-inch helium tunnel	8	16.2	.79	.31	51.7	75.0	306	550	2.8	.05	.02	Transitional at $x \approx 353$ cm (139 in.)
Langley 4-inch Mach 5 nozzle	11	5.0	1.02	.40	34.5	50.0	378	610	6.0	8.2	2.5	} Cold wall; transitional near exit
	and	↓	↓	↓	41.5	60.0	↓	↓	7.2	9.8	3.0	
	appendix	↓	↓	↓	48.3	70.0	↓	↓	8.4	11.4	3.5	Hot wall; transitional near exit
Langley rapid-expansion nozzle		5.0	1.02	.40	34.5	50.0	378	610	6.0	8.2	2.5	Transitional at $x \approx 38$ cm (15 in.)
Nash-Webber nozzle A	39	≈2.0	5.73	2.26	1.7	2.5	286	515	2.4	2.2	.7	Laminarized upstream of
		≈2.0	5.73	2.26	3.4	5.0	289	520	4.1	4.4	1.3	nozzle throat
JPL conical nozzles:	‡16											
10° approach		≈3.7	2.01	.79	16.1	21.0	830	1500	1.7	1.7	.5	Laminarized upstream of
45° approach		≈4.0	2.01	.79	39.8	52.0	830	1500	4.2	3.5	1.1	nozzle throat

*Also private communication from J. M. Kendall at Jet Propulsion Laboratory.

†Also private communication from J. L. Amick at the University of Michigan.

‡Based on heat-transfer data of figure 3 of reference 16.

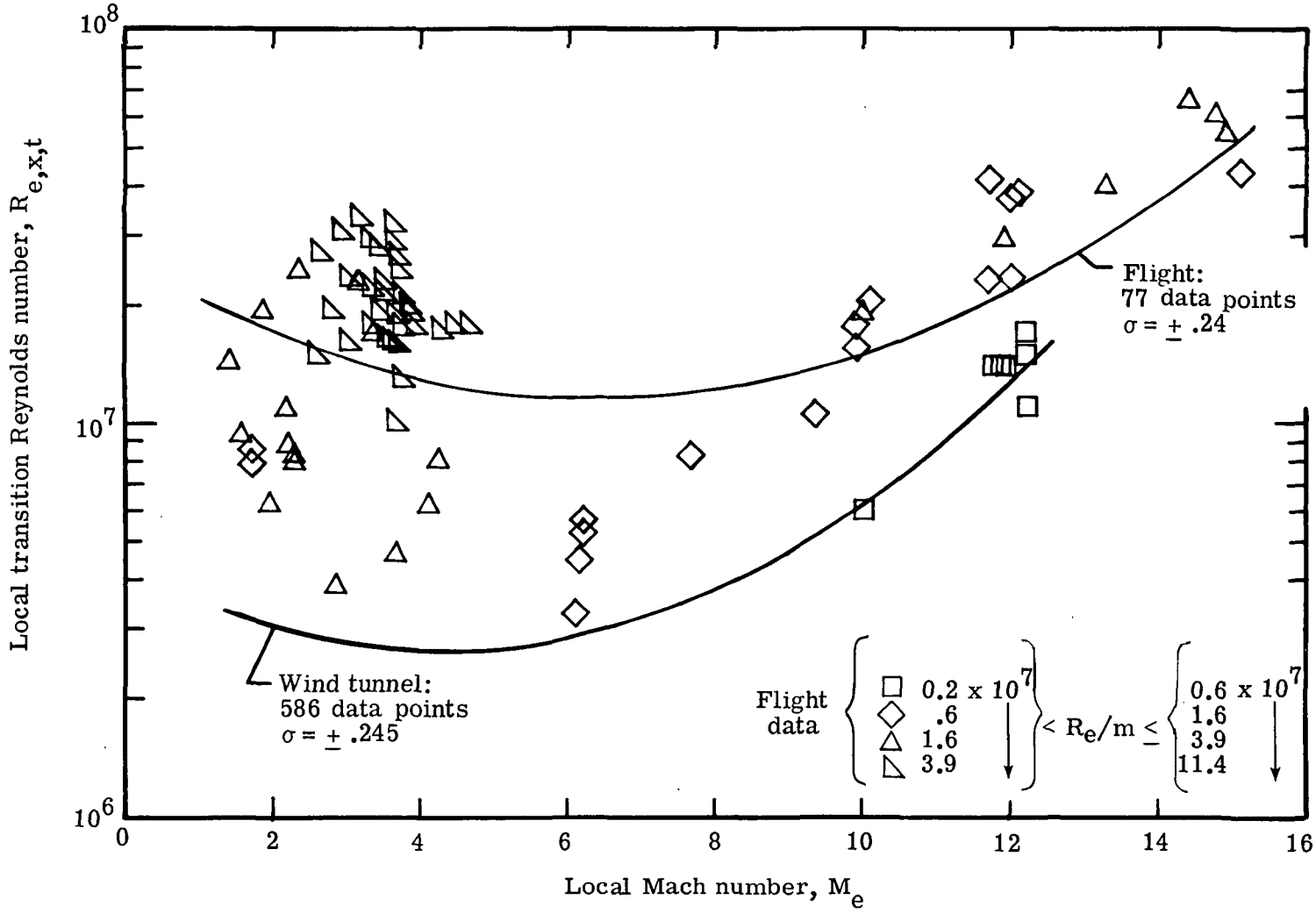

Figure 1.- Comparison of least-squares correlations for transition data on sharp cones at small angles of attack.

Coordinates in Table I -	Case		Ref.	M	p_o		T_o		T_w		y_*	
					psia	N/cm^2	°R	K	°R	K	in.	cm
(a)	1	JPL 20-inch	7	4.6	7.7	5.3	530	295	T_{aw}		0.555	1.41
(b)	2	22-inch He(LaRC)	8	16.2	75	51.7	550	306	T_{aw}		.31	.79
(c)	3	6.6-inch Mach 8 Univ. of Mich.	37	8	90	62.1	1260	700	530	294	.22	.56
(d)	4	4-inch Mach 5	11	5	50	34.5	680	378	T_{aw}		.40	1.02
(e)	5	Rapid expansion	Pres.	5	50	34.5	680	378	T_{aw}		.40	1.02

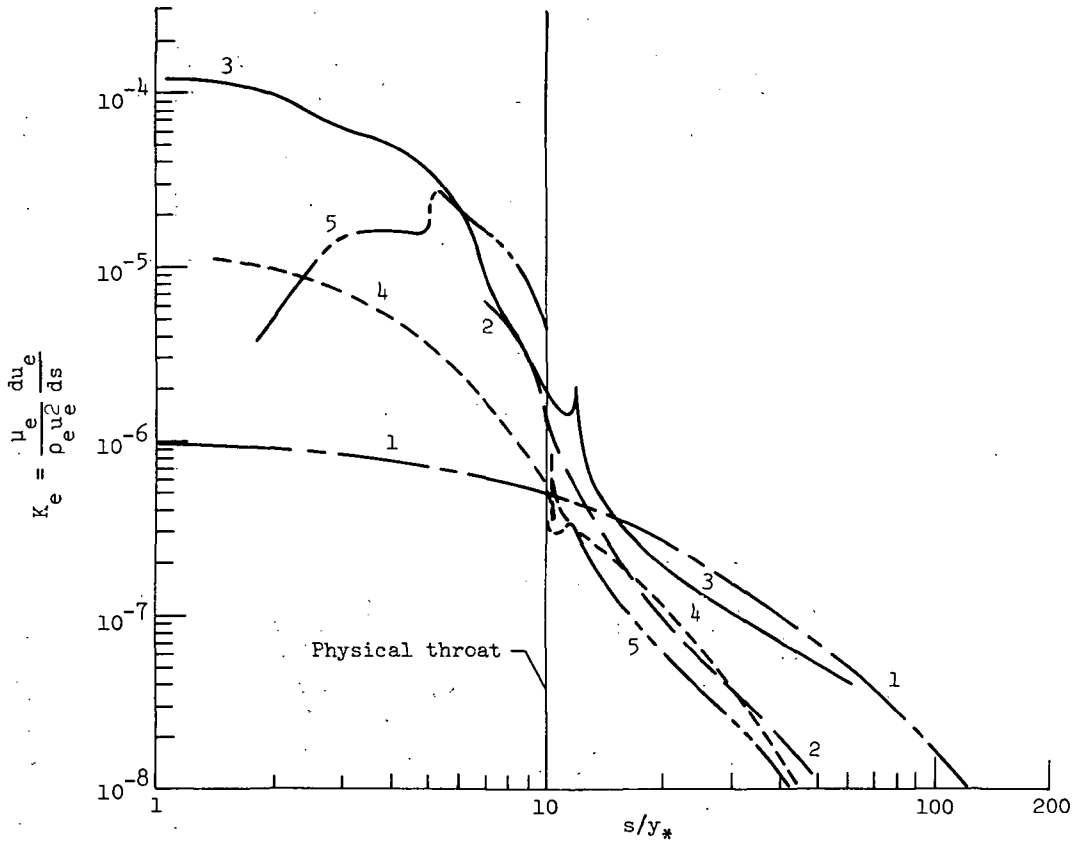

(a) Gas parameters evaluated in local free stream.

Figure 2.- Variation of laminarization parameters in supersonic nozzles with laminar boundary layers.

Coordinates in Table I -	Case		Ref.	M_∞	p_o psia	p_o N/cm^2	T_o °R	T_o K	T_w °R	T_w K	y_* in.	y_* cm
(a)	1	JPL 20-inch	7	4.6	7.7	5.3	530	295	T_{aw}		0.555	1.41
(b)	2	22-inch He (LaRC)	8	16.2	75	51.7	550	306	T_{aw}		.31	.79
(c)	3	6.6-inch Mach 8 Univ. of Mich.	37	8	90	62.1	1260	700	530	294	.22	.56
(d)	4	4-inch Mach 5	11	5	50	34.5	680	378	T_{aw}		.40	1.02
(e)	5	Rapid expansion (LaRC)	Pre-sent	5	50	34.5	680	378	T_{aw}		.40	1.02
	6a	Nash-Webber nozzle A	39	2	2.5	1.7	515	286	T_{aw}		2.26	5.73
	6b	Nash-Webber nozzle A	39	2	5.0	3.4	520	259	T_{aw}		2.26	5.73

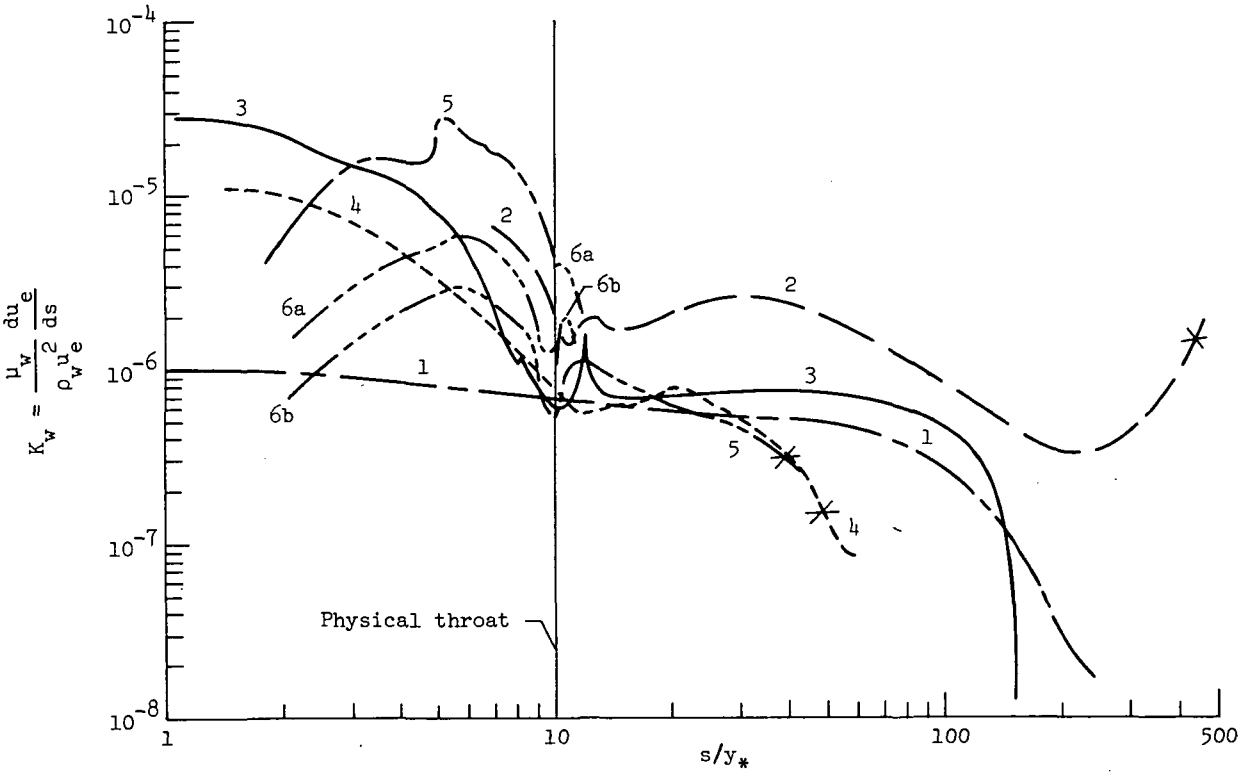

(b) Gas properties evaluated at wall. Approximate location of transition indicated by X.

Figure 2.- Concluded.

Coordinates in Table I -	Case		Ref.	M_∞	p_o psia	p_o N/cm^2	T_o °R	T_o K	T_w °R	T_w K	y_* in.	y_* cm
(a)	1	JPL 20-inch	7	4.6	7.7	5.3	530	295	T_{aw}		0.555	1.41
(b)	2	22-inch He (LaRC)	8	16.2	75	51.7	550	306	T_{aw}		.31	.79
(c)	3	6.6-inch Mach 8 Univ. of Mich.	37	8	90	62.0	1260	700	530	294	.22	.56
(d)	4	4-inch Mach 5 (LaRC)	11	5	50	34.5	680	378	T_{aw}		.40	1.02
(e)	5	Rapid expansion		5	50	34.5	680	378	T_{aw}		.40	1.02
	Design 6	Slotted nozzle	Pre-sent	5	50	34.5	680	378	T_{aw}		.50	1.27
	Design 6a	Slotted nozzle		5	200	138	680	378	T_{aw}		.50	1.27

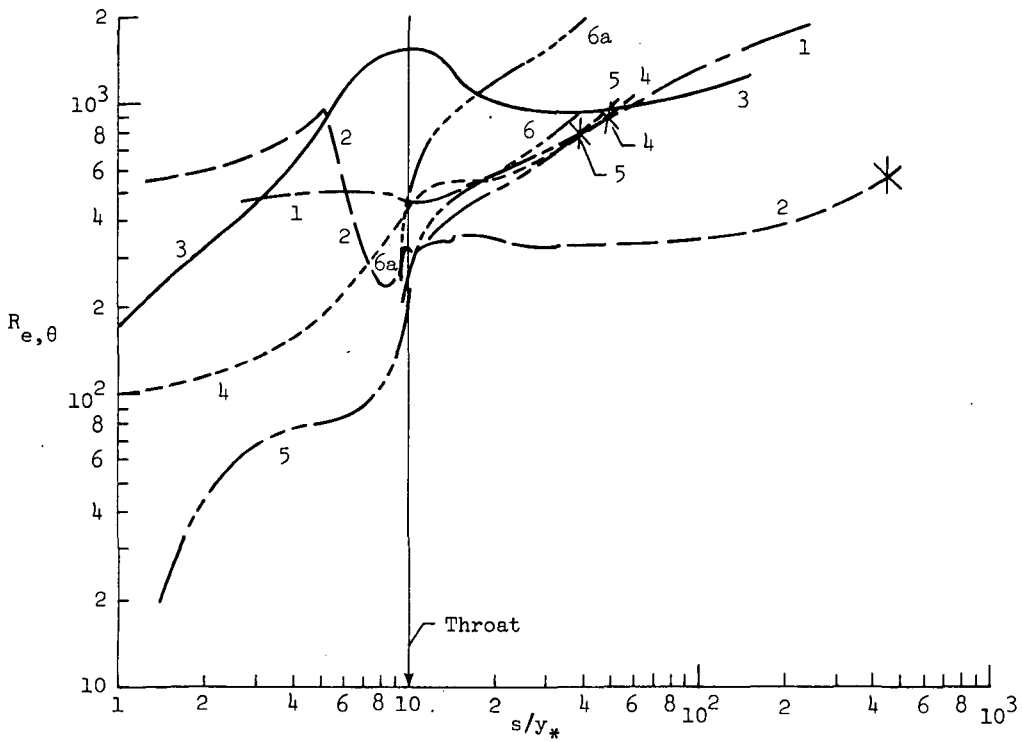

Figure 3.- Variation of momentum thickness Reynolds numbers in supersonic nozzles with laminar boundary layers (except slotted nozzle which has not yet been tested). Approximate location of transition indicated by X.

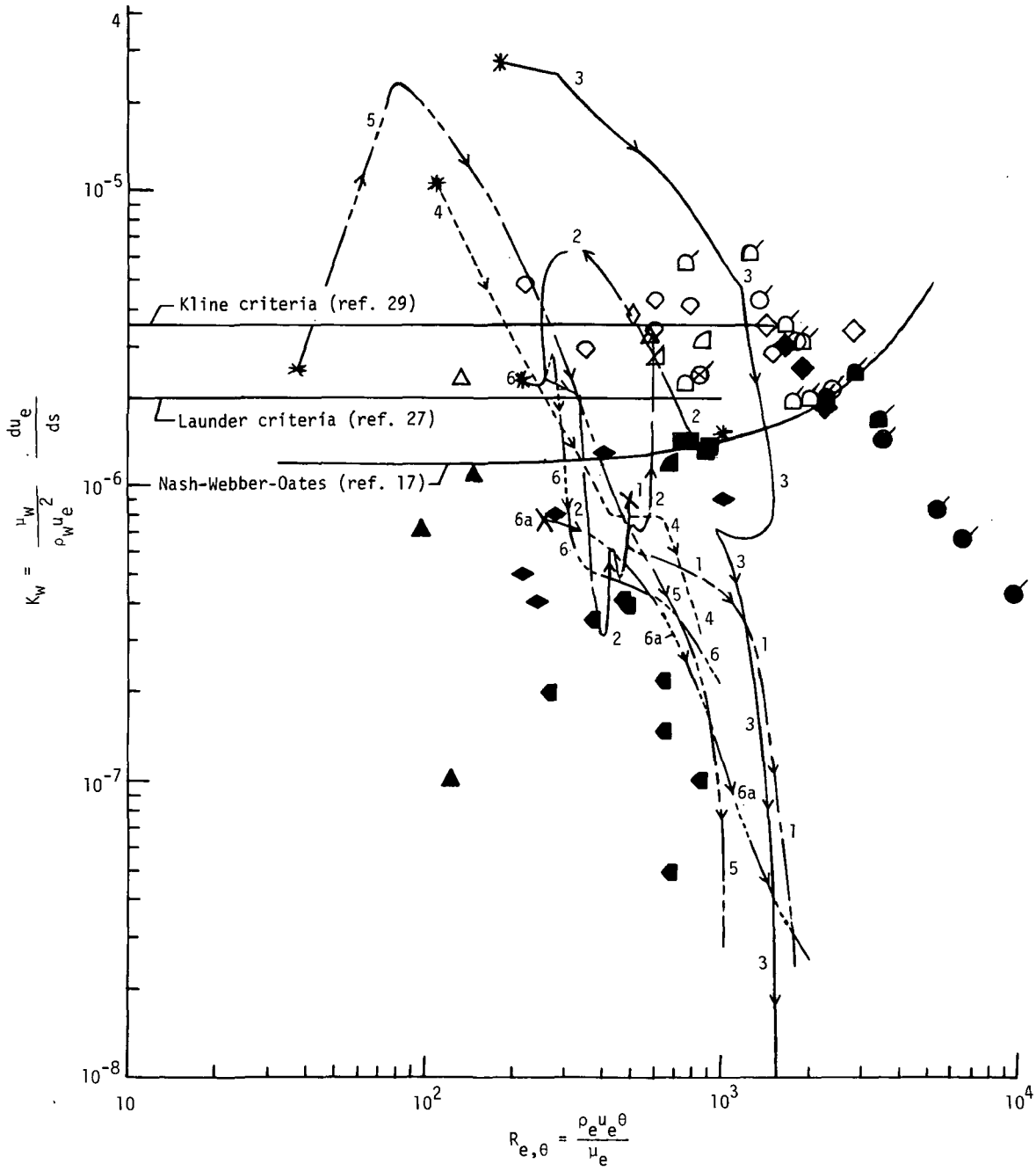

(a) Plot.

Figure 4.- Variation of K_w with $R_{e,\theta}$ for laminar boundary layers in nozzles and for relaminarization of initially turbulent layers. Wall temperature was approximately adiabatic for all cases except references 16 and 37 where T_w/T_t was 0.42 to 0.50, and 0.42, respectively. Open symbols denote relaminarized boundary layers; closed symbols denote fully turbulent boundary layers. Flagged symbols denote data in the subsonic approach of nozzles.

Case	Symbol	Reference	Test apparatus	M_e	Comments
1	— — —	7	JPL 20-inch tunnel	4.6	Laminar for full nozzle length
2	—— ——	8	22-inch helium tunnel (LaRC)	16.2	Laminar up to exit region
3	———	37	Univ. of Michigan	8	Laminar for full nozzle length
4	- - - - - -	11	4-inch Mach 5	5	Laminar for two-thirds of length
5	—— - - ——	Present	Rapid expansion (LaRC)	5	Laminar for two-thirds of length
6	—— - - - ——	Present (Design)	Slotted (LaRC)	5	p_o = 50 psia } Test results not
6a	—— - · - ——	Present (Design)	Slotted (LaRC)	5	p_o = 200 psia } yet available
	○	16	Conical nozzle	M < 1.0	} Boundary layers upstream of
	⊗	45	Conical nozzle	0.19	} approach were turbulent
	□	42	2-D channel	Incompressible	
	◇	28	2-D channel	Incompressible	
	△	44	Centerbody in axisymmetric nozzle	0.21 to 0.97	Data in nozzle approach only
	◿	29	2-D channel	Incompressible	
	◿	27	2-D channel	Incompressible	
	∩	17	Nozzles A, B, and C	M < 1.0	Assumed $\frac{u_e\theta}{\nu_w} \approx \frac{u_e\theta}{\nu_e}$
	⬡	30	2-D channel	Incompressible	
	◊	43	Turbine blades	Incompressible	
	◇ } ◿ }	46	Nozzle (curved wall) Nozzle (flat wall)	0.48 to 2.01 0.48 to 2.01	Max. $K \approx 1.3 \times 10^{-6}$

(b) Key.

Figure 4.- Concluded.

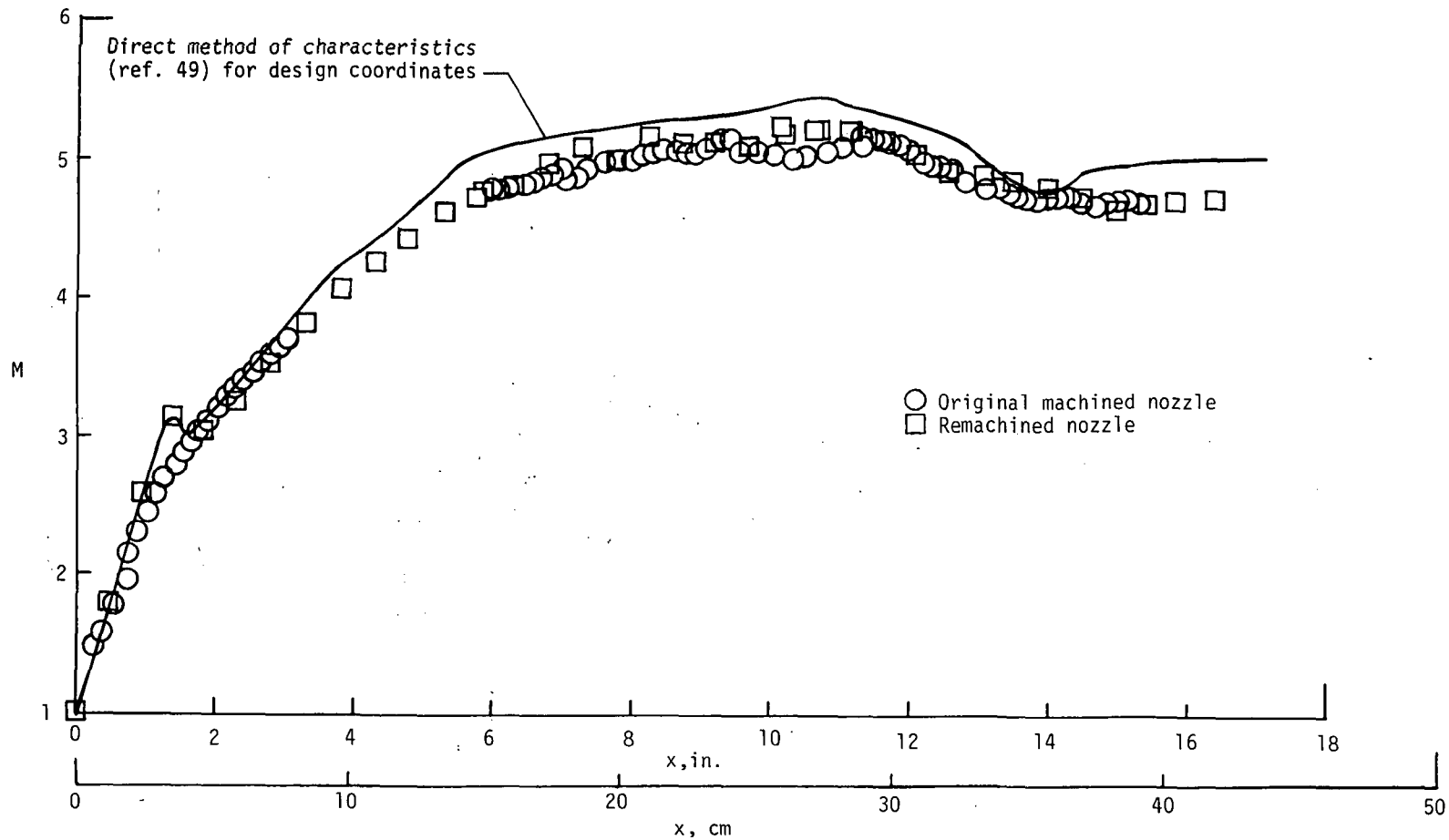

Figure 5.- Mach number distribution along center line of rapid-expansion nozzle.

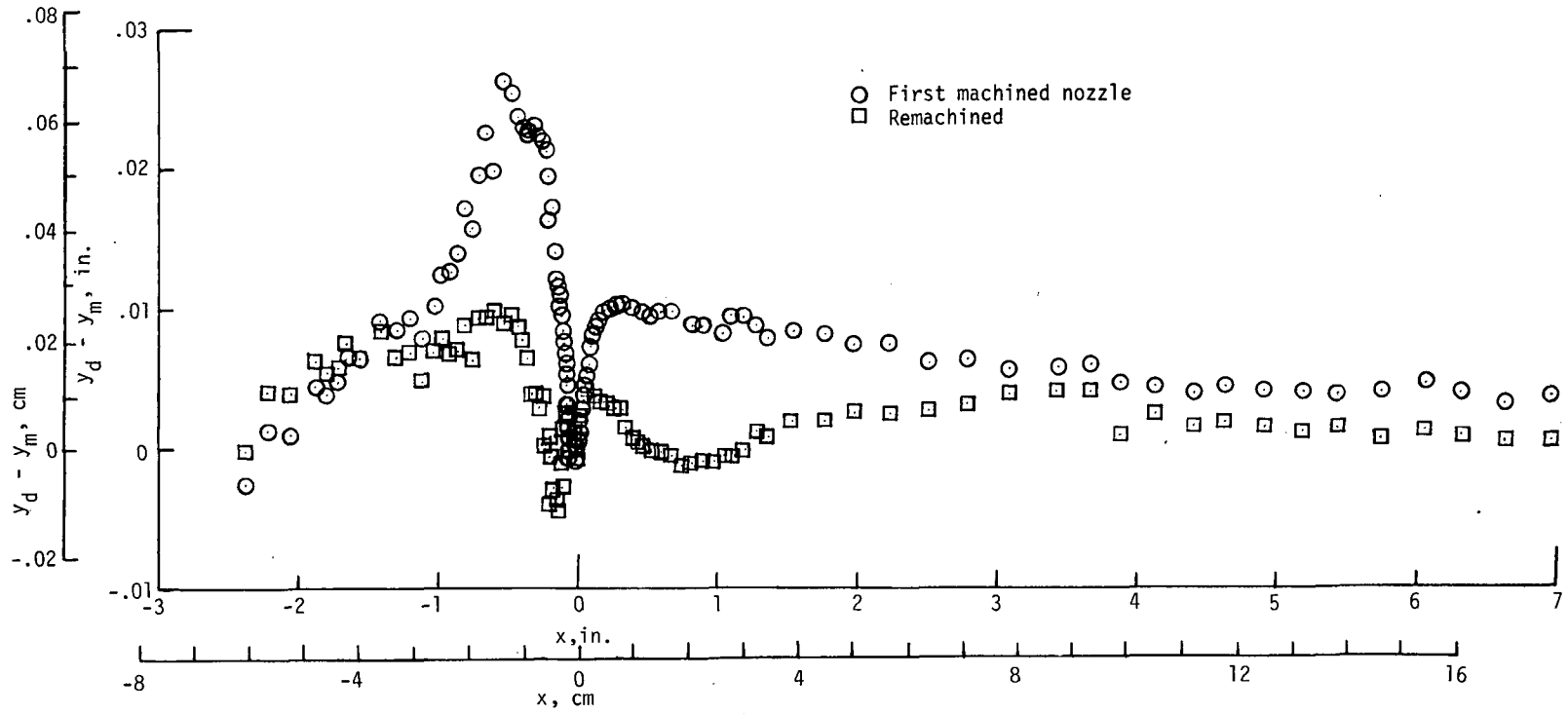

Figure 6.- Machining discrepancies for the rapid-expansion nozzle.

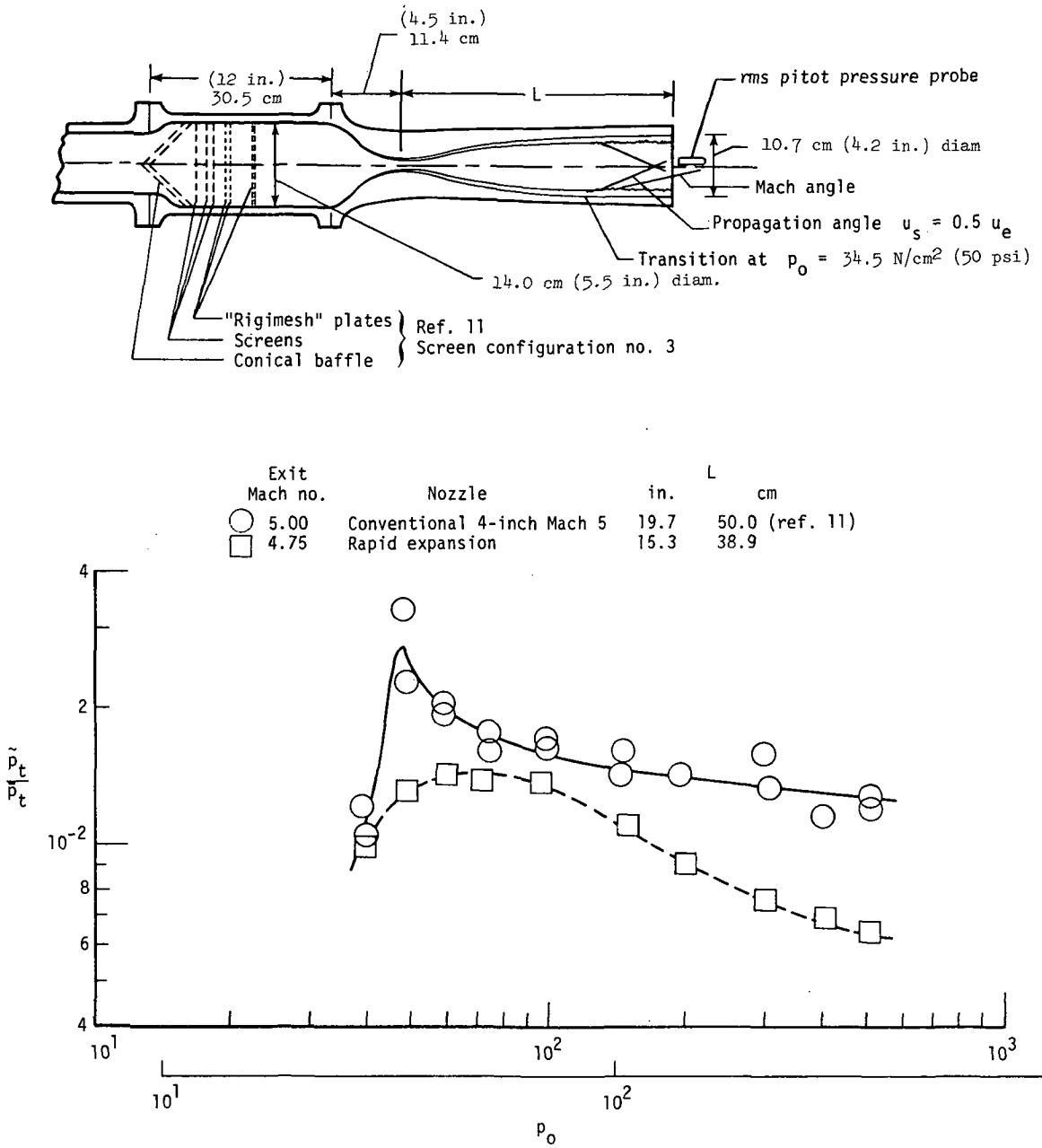

Figure 7.- Root-mean-square pitot pressure in the conventional 4-inch Mach 5 nozzle and in the rapid-expansion nozzle. (Exit diameter of both nozzles is 10.7 cm (4.2 in.).)

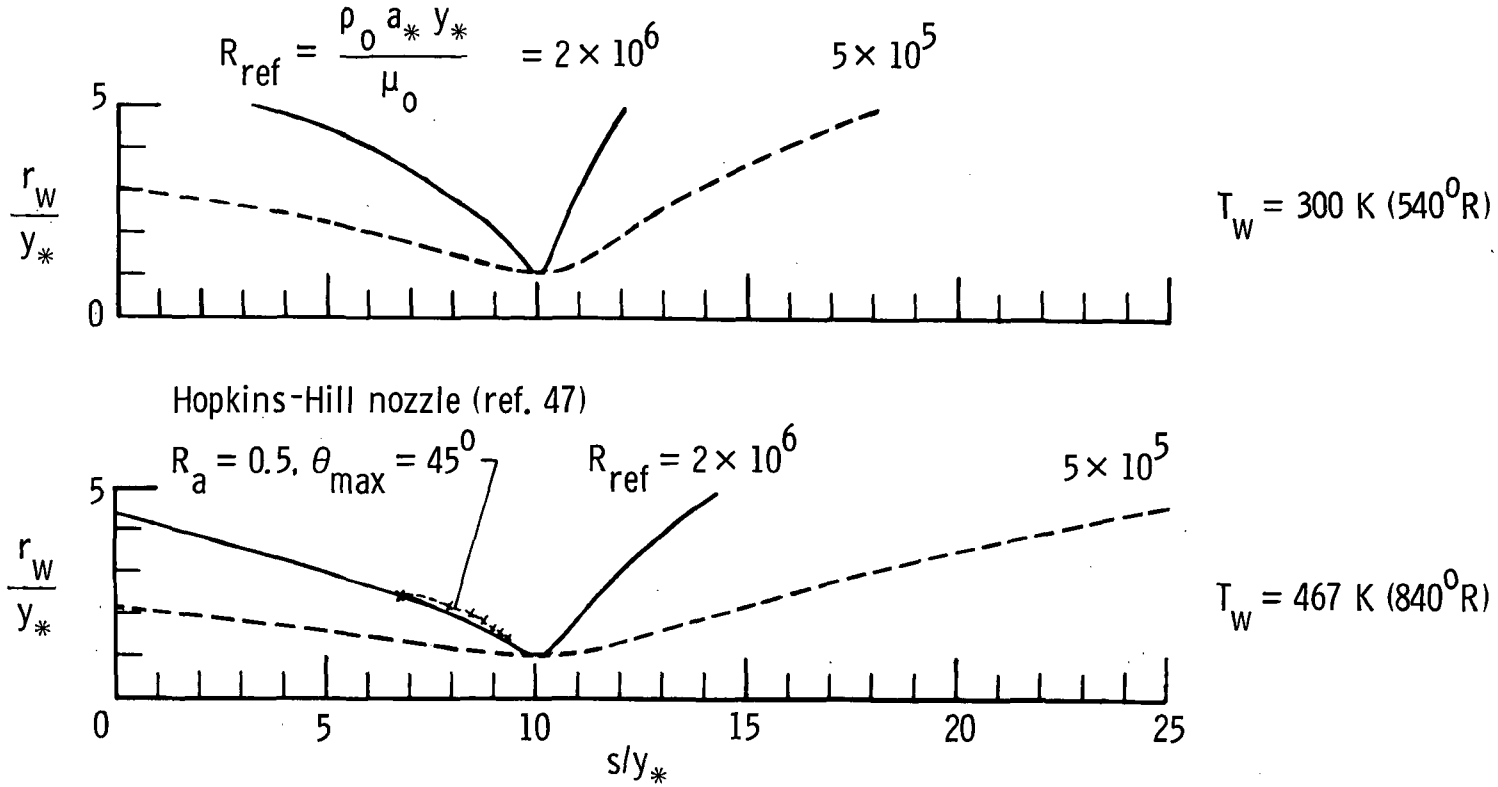

Figure 8.- One-dimensional nozzle shapes for $K_w = \frac{\mu_w \frac{du_e}{ds}}{\rho_w u_e^2} = 2 \times 10^{-6}$.

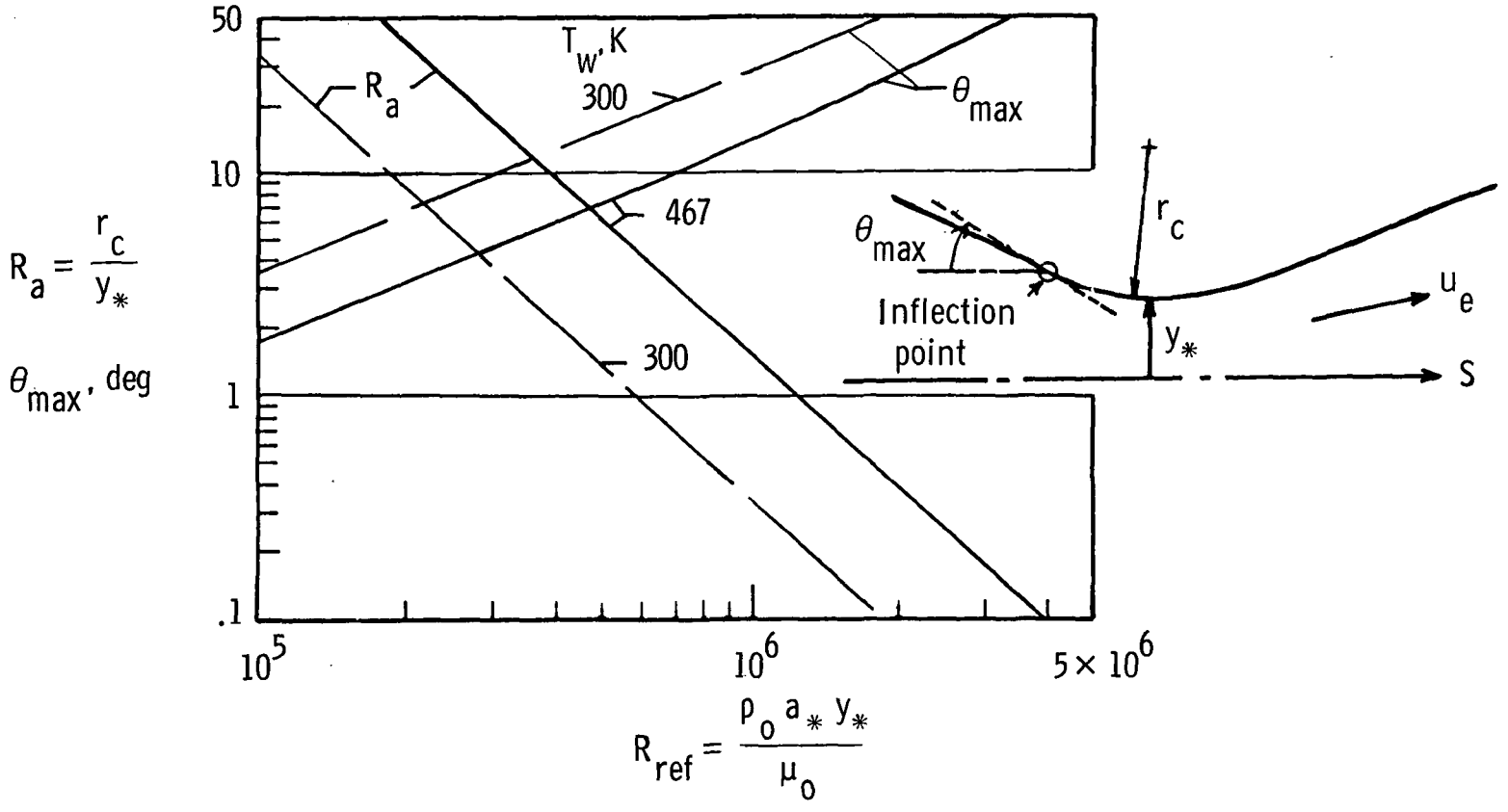

Figure 9.- Values of one-dimensional nozzle parameters required for $K_w = \frac{\mu_w \frac{du_e}{ds}}{\rho_w u_e^2} = 2 \times 10^{-6}$.

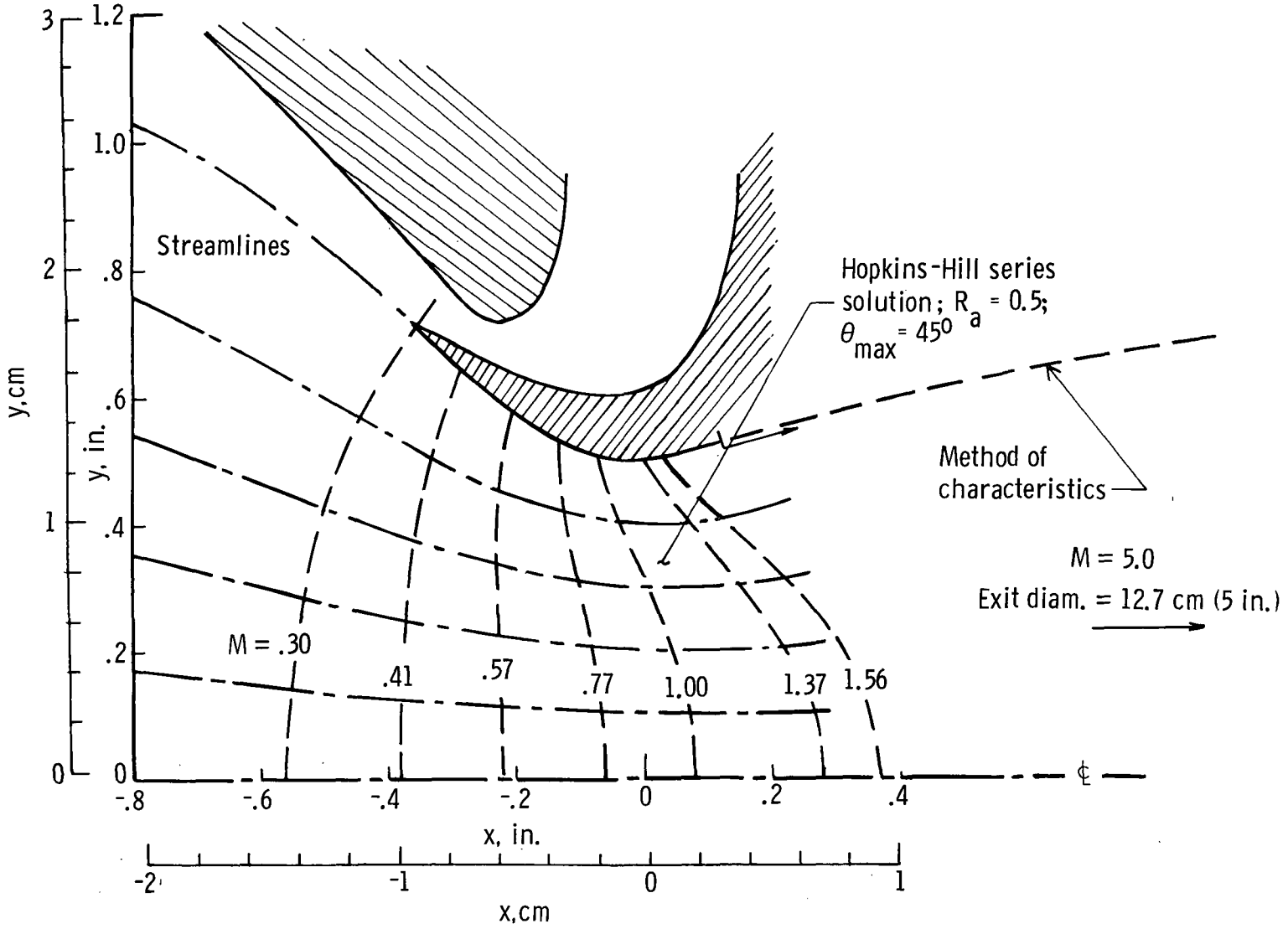

Figure 10.- Typical slotted-throat design for laminar flow nozzle.

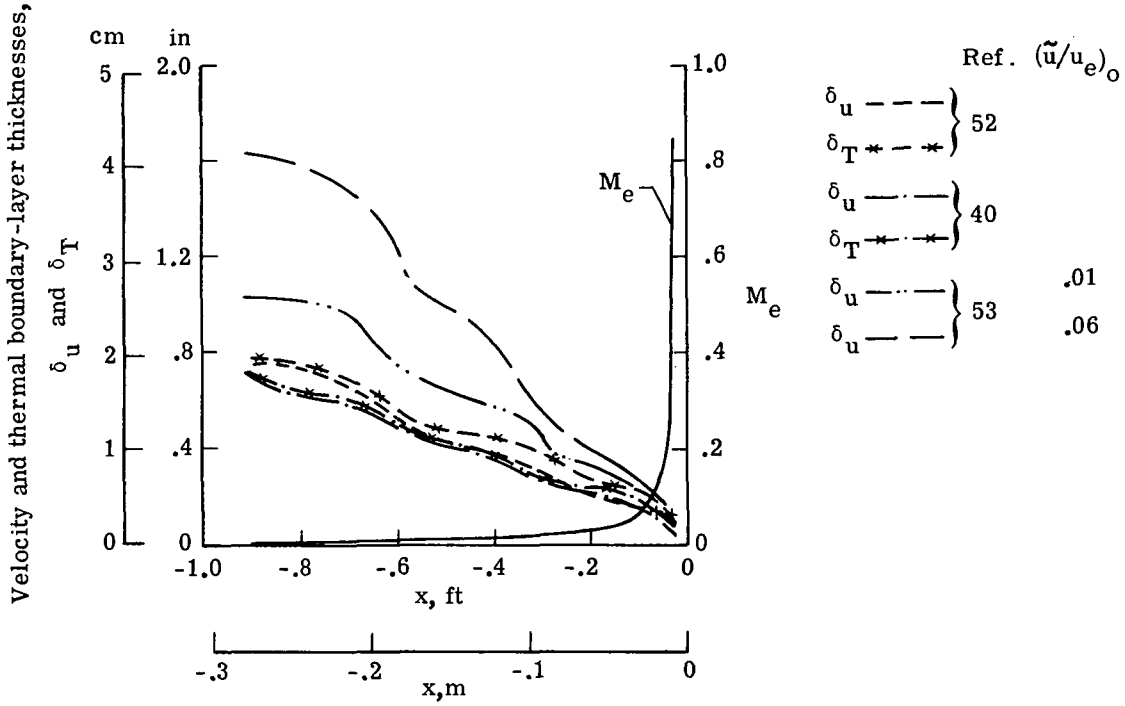

(a) δ_u and δ_T for entire subsonic approach.

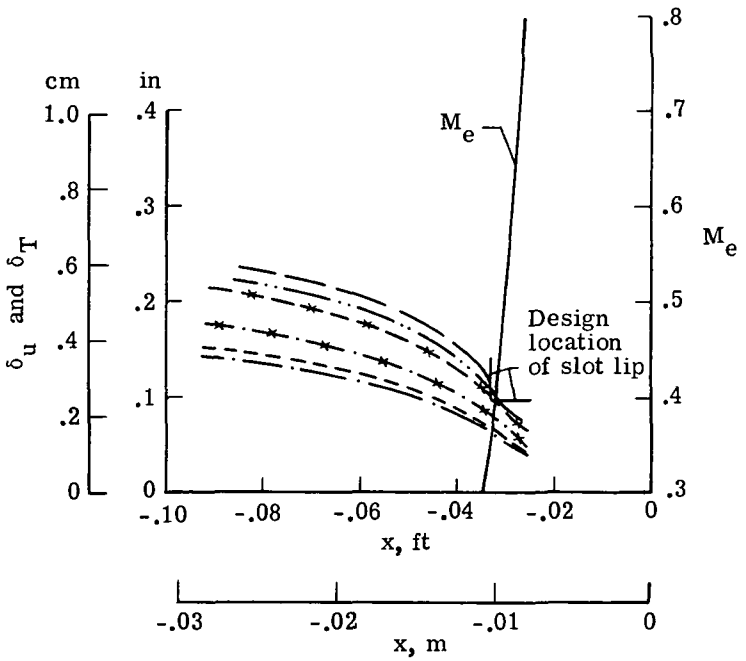

(b) δ_u and δ_T in vicinity of suction slot.

Figure 11.- Boundary-layer parameters in subsonic approach of Mach 5 slotted nozzle. $R_a = 1.0$; $\theta_{max} = 45^o$; $p_o = 103.5$ N/cm^2 (150 psia).

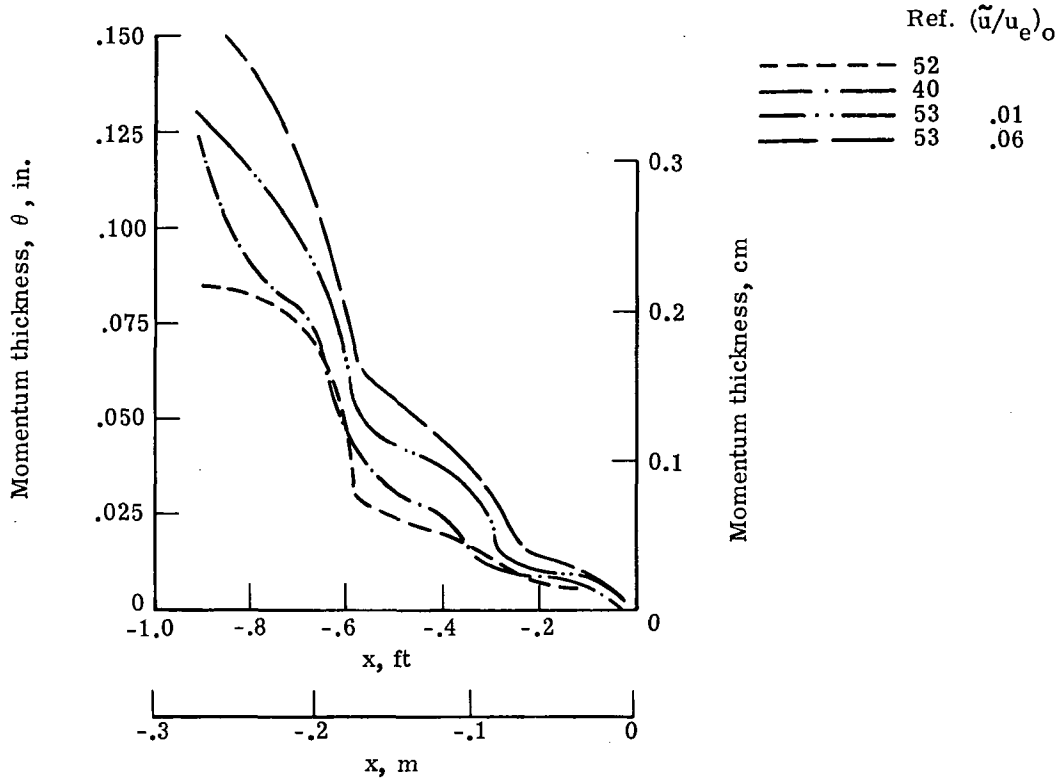

(c) Momentum thickness.

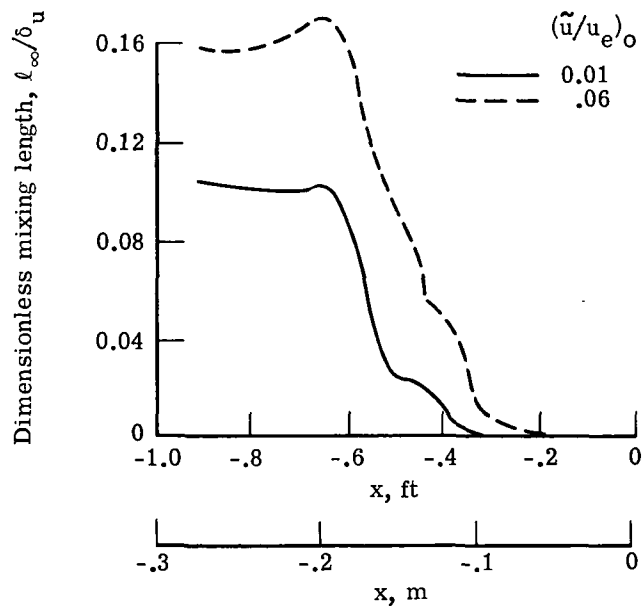

(d) Dimensionless mixing length computed by the method of reference 53.

Figure 11.- Concluded.

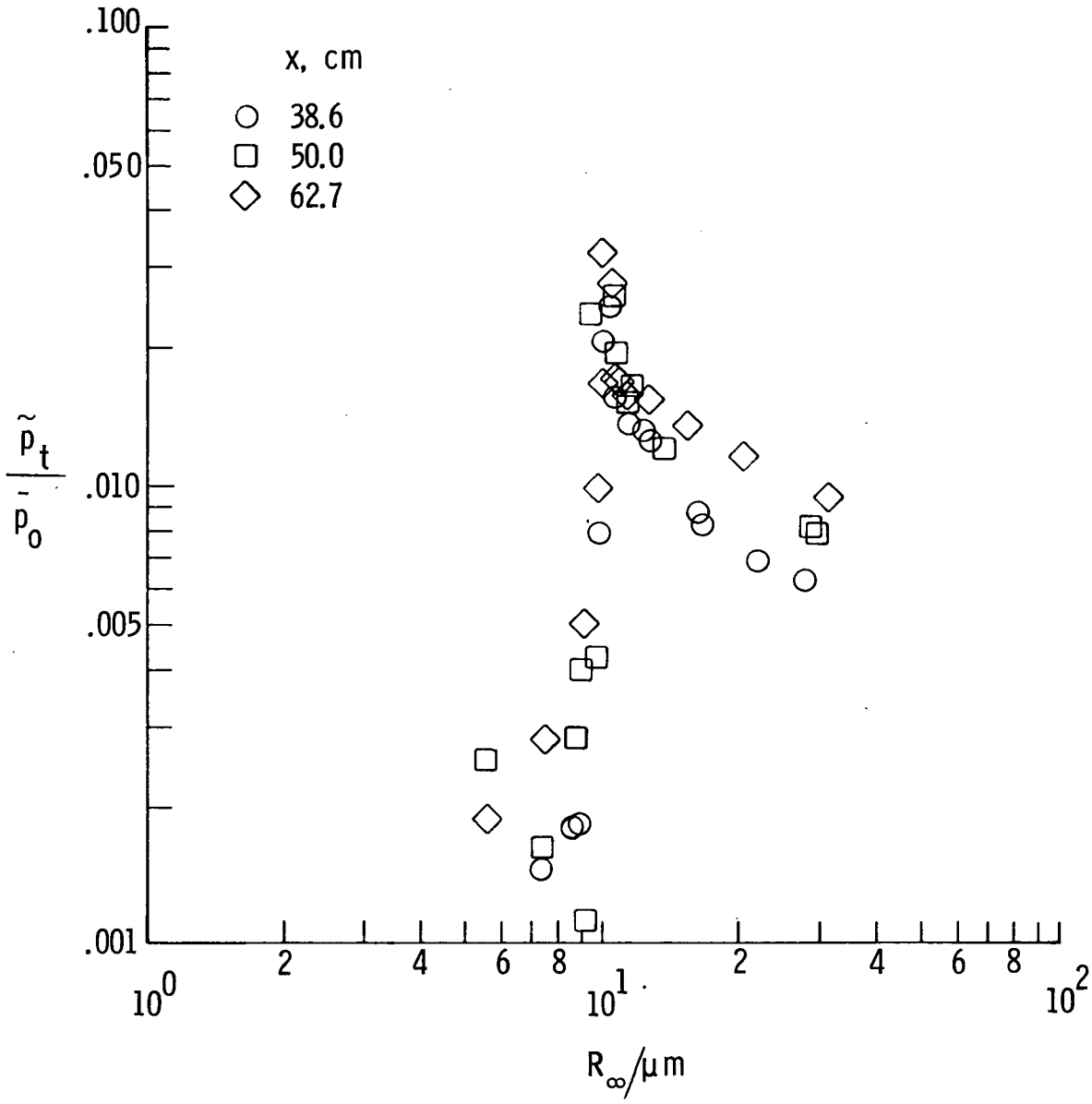

Figure 12.- Fluctuating pitot pressure for smooth nozzle. Probe 1.27 cm above tunnel center line.

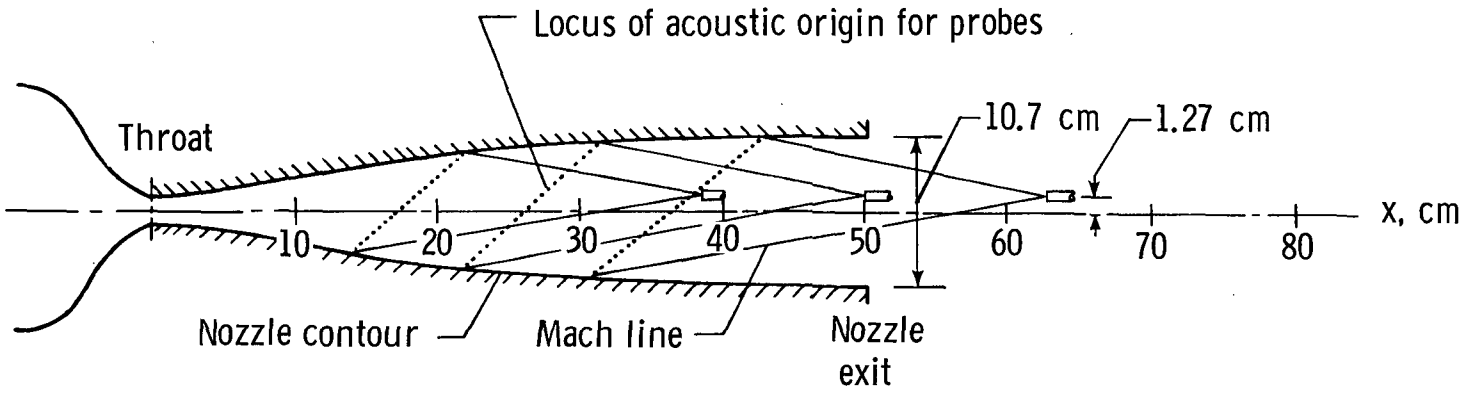

Figure 13.- Acoustic origin of disturbances measured by probes.

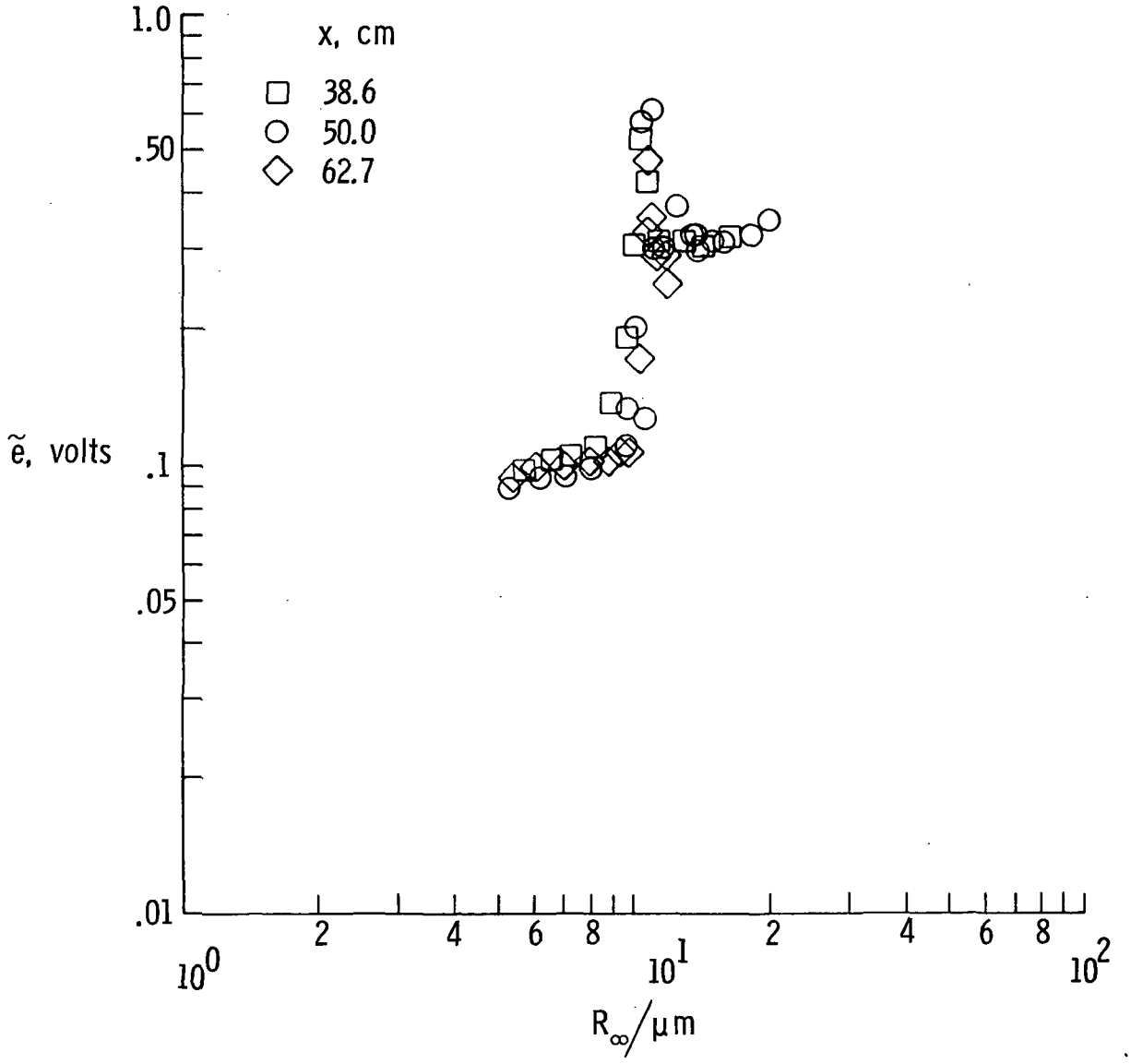

Figure 14.- Hot-wire root-mean-square signal 1.27 cm above tunnel center line.

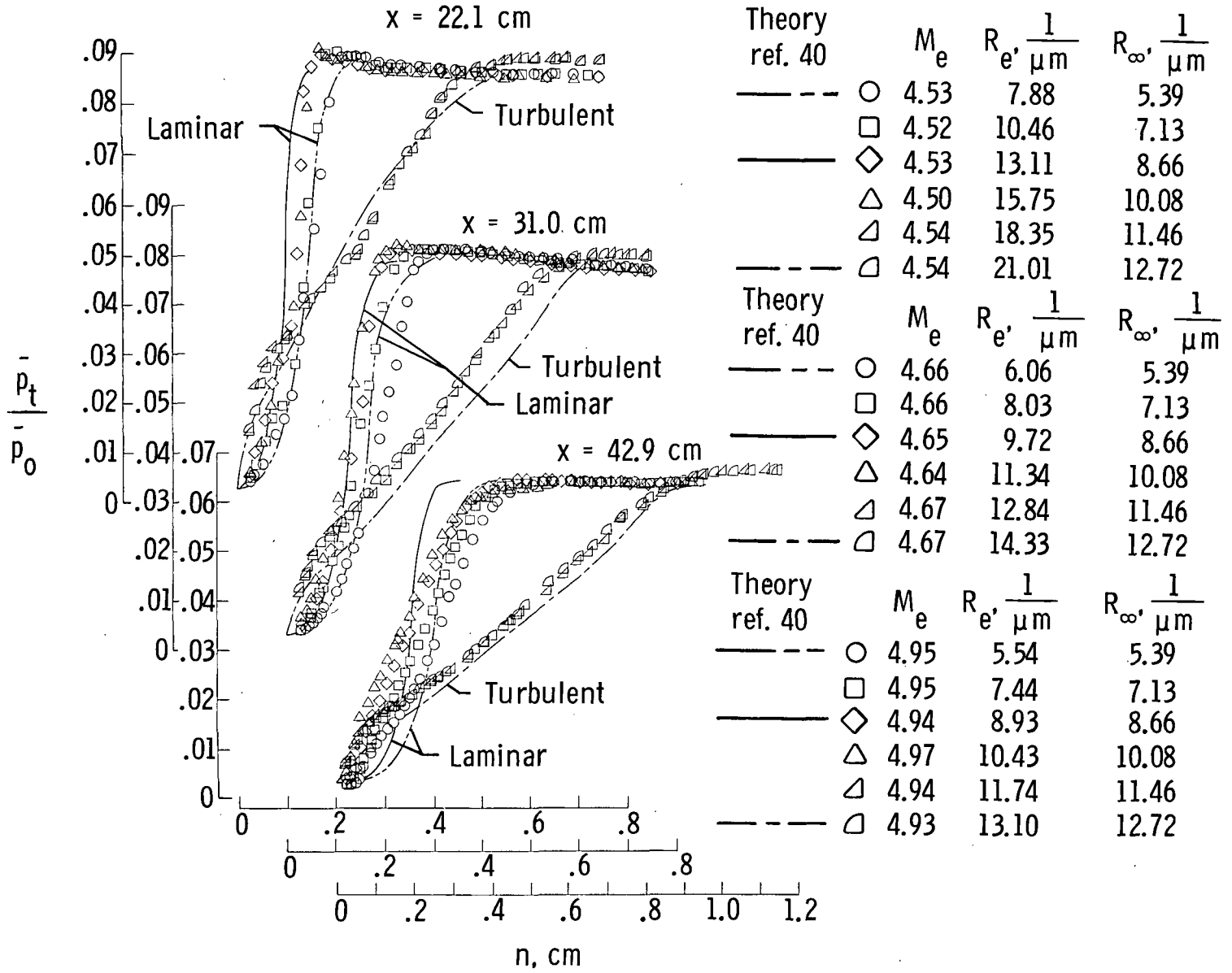

Figure 15.- Boundary-layer profiles compared with theory.

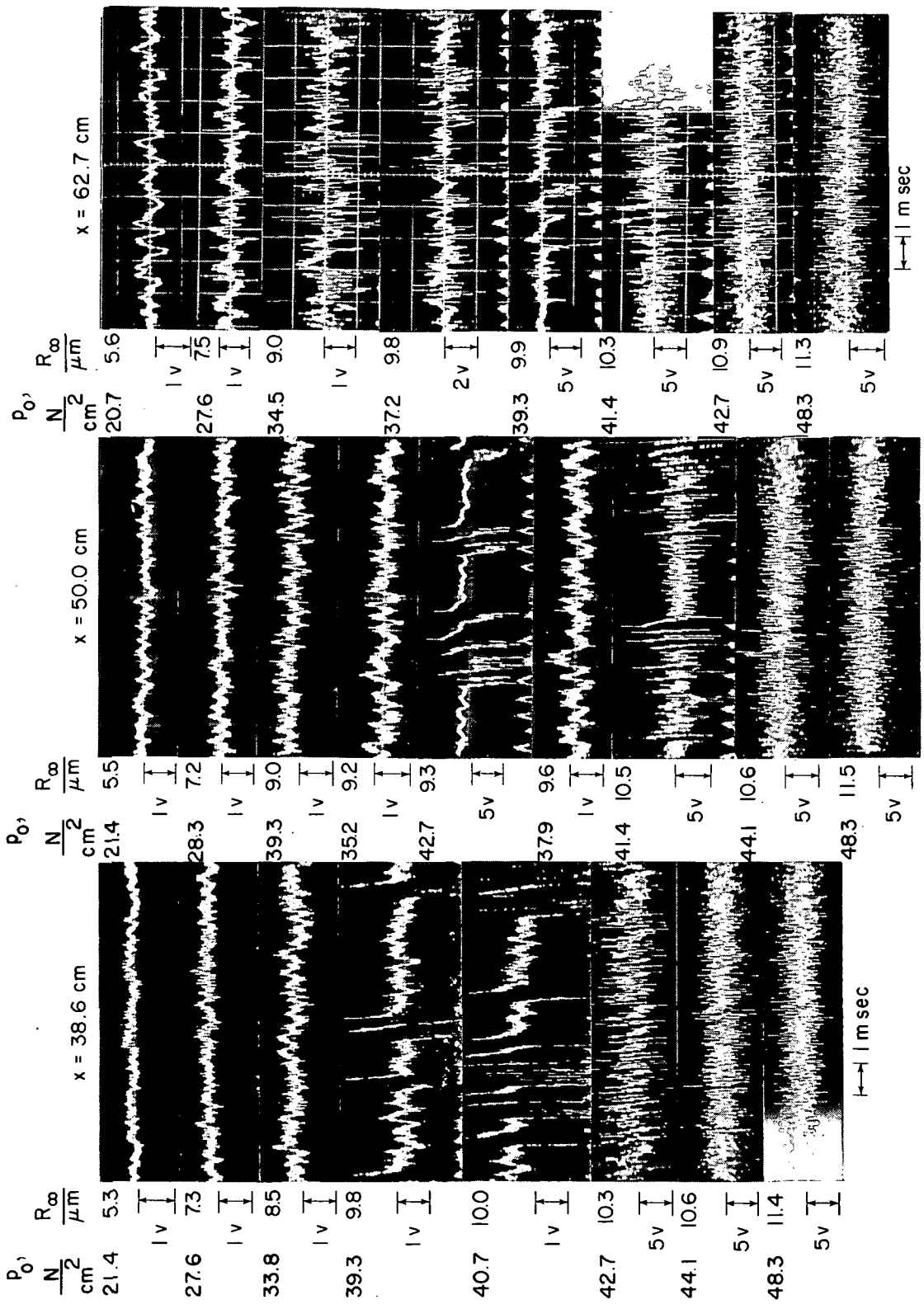

Figure 16.- Oscilloscope traces of the output (in volts) from pressure transducer.

NATIONAL AERONAUTICS AND SPACE ADMINISTRATION
WASHINGTON, D.C. 20546

OFFICIAL BUSINESS
PENALTY FOR PRIVATE USE $300

SPECIAL FOURTH-CLASS RATE BOOK

POSTAGE AND FEES PAID
NATIONAL AERONAUTICS AND SPACE ADMINISTRATION
451

U.S.MAIL

POSTMASTER: If Undeliverable (Section 158 Postal Manual) Do Not Return

"The aeronautical and space activities of the United States shall be conducted so as to contribute . . . to the expansion of human knowledge of phenomena in the atmosphere and space. The Administration shall provide for the widest practicable and appropriate dissemination of information concerning its activities and the results thereof."

—NATIONAL AERONAUTICS AND SPACE ACT OF 1958

NASA SCIENTIFIC AND TECHNICAL PUBLICATIONS

TECHNICAL REPORTS: Scientific and technical information considered important, complete, and a lasting contribution to existing knowledge.

TECHNICAL NOTES: Information less broad in scope but nevertheless of importance as a contribution to existing knowledge.

TECHNICAL MEMORANDUMS: Information receiving limited distribution because of preliminary data, security classification, or other reasons. Also includes conference proceedings with either limited or unlimited distribution.

CONTRACTOR REPORTS: Scientific and technical information generated under a NASA contract or grant and considered an important contribution to existing knowledge.

TECHNICAL TRANSLATIONS: Information published in a foreign language considered to merit NASA distribution in English.

SPECIAL PUBLICATIONS: Information derived from or of value to NASA activities. Publications include final reports of major projects, monographs, data compilations, handbooks, sourcebooks, and special bibliographies.

TECHNOLOGY UTILIZATION PUBLICATIONS: Information on technology used by NASA that may be of particular interest in commercial and other non-aerospace applications. Publications include Tech Briefs, Technology Utilization Reports and Technology Surveys.

Details on the availability of these publications may be obtained from:

SCIENTIFIC AND TECHNICAL INFORMATION OFFICE

NATIONAL AERONAUTICS AND SPACE ADMINISTRATION

Washington, D.C. 20546